



UNIVERSITAT POLITÈCNICA DE CATALUNYA
BARCELONATECH
Escola d'Enginyeria de Barcelona Est

MASTER THESIS

Master in Chemical Engineering

**AUTOMATED ONLINE AND REAL-TIME MONITORING OF
ENVIRONMENTAL RISK**



Thesis and annexes

Author: Josep Rovira Segarra
Director: Antonio Florido
Convocation: June 2018

Resum

Actualment la degradació del medi ambient per mitjà de l'acció humana ha creat la necessitat de monitoritzar les aigües residuals industrials, rius i oceans per a una detecció ràpida, in situ i a temps real dels contaminants. Aquest treball pretén optimitzar un sistema de detecció de metalls pesants basat en diferents Elèctrodes Selectius de Ions (ISE) implantats en un equip d'Anàlisi per Injecció Seqüencial (SIA) per la auto-preparació de patrons químics, calibratge i anàlisi de mostres en un sol equip. L'objectiu és calibrar, optimitzar i automatitzar diferents ISE implantats en una sola unitat, normalment anomenada Llengua Electrònica (ET), degut a la comparació amb la funcionalitat de la llengua biològica. En aquest treball s'ha aconseguit amb èxit la instal·lació de ISEs en un equip automatitzat, el calibratge dels elèctrodes i la correcta determinació de metalls. També la millora de la qualitat del senyal mitjançant la identificació de fonts de soroll. S'ha estudiat un sistema de monitorització online. Es consideren els Protocols de Transferència Segura de Dades (SFTP) com una opció factible per la monitorització a través de la xarxa i amb anàlisi a temps real en la Base de Dades per l'Anàlisi de Risc (RAdb) desenvolupada per el Institut Noruec de la Investigació de l'Aigua (NIVA).

Resumen

Actualmente la degradación del medio ambiente por medio de la acción humana ha creado la necesidad de monitorizar las aguas residuales industriales, ríos y océanos para una detección rápida, in situ y a tiempo real de contaminantes. El presente trabajo pretende optimizar un sistema de detección de metales pesados basado en diferentes Electroodos Selectivos de Iones (ISE) implantados en un equipo de Análisis por Inyección Secuencial (SIA) para la auto-preparación de patrones químicos, calibración y análisis de muestras en un mismo equipo. El objetivo es calibrar, optimizar y automatizar diferentes ISE implantados en una sola unidad, normalmente descrita como Lengua Electrónica (ET), debido a la comparación con la funcionalidad de la lengua biológica. En este trabajo se ha logrado con éxito la instalación de ISEs en un equipo automatizado, la calibración de los electrodos y la correcta determinación de metales. También a mejora de la calidad de la señal mediante la identificación de las fuentes de ruido. Se ha estudiado un sistema de monitorización online. Se considera a los Protocolos de Transferencia Segura de Datos (SFTP) como una opción factible para la monitorización a través de la red y con análisis a tiempo real en la Base de Datos para el Análisis del Riesgo (RAdb) desarrollada por el Instituto Noruego de la Investigación del Agua (NIVA).

Abstract

Currently the environment degradation due to human activities created the need of monitoring the industrial waste waters, rivers and oceans for fast, on site and real-time pollutants detection. The present work intends to optimize a heavy metals detection system based on different Ion Selective Electrodes (ISE) implanted in a Sequential Injection Analysis (SIA) equipment for self-preparation of chemical patterns, calibration and sample analysis in a single equipment. The goal is to calibrate, optimize and automate different ISE implanted in a single unit, usually described as an Electronic Tongue (ET) in the literature, due to its comparison with biological tongue functionality. In this work the setup of the ISEs within an automated system, the calibration of the electrodes and the determination of metals was achieved successfully. Also, the improvement of quality signal is achieved by identifying the noise sources. The study of an online monitoring system is investigated. The Secure File Transfer Protocols (SFTP) are considered as a suitable option for online monitoring and real time analysis with the Risk Assessment Data Base (RAdb), developed by the Norwegian Institute for Water Research (NIVA).

Acknowledgements

I would like to acknowledge the invaluable help of Dr. Antonio Florido for his advice and guidance during the realization of this project. To Dr. Alexandra Espriu and PhD student Karina Torres for the support received and the expertise they shared. Additionally, I would like to thank Paula García, for her amazing help during the development of the project and all the hard work done. Thanks to Dr. Knut Erik Tollefsen, Hans-Christian Tollefsen and Yang Li from the NIVA research centre for making our collaboration so fruitful and having the great idea of connecting both projects. Finally, I want to thank the inestimable support and patience of my wife, without whom I could have not achieved the realization of this project.

Glossary

UPC	“Universitat Politècnica de Catalunya” (Polytechnic University of Catalunya)
EEBE	“Escola d’Enginyeria de Barcelona Est” (Est Barcelona Engineering School)
SIA	Sequential Injection Analysis
FIA	Flow Injection Analysis
ISE	Ion Selective Electrode
ET	Electronic Tongue
FAAS	Flame Atomic Absorption Spectroscopy
ICP-OES	Inductively Coupled Plasma Optical Emission Spectrometry
LOD	Limit of Detection
FIM	Fixed Interference Method
NIVA	Norwegian Institute for Water Research
RAdb	Risk Assessment Database
MOA	Mode of Action
MOE	Margin of error (%)
DOS	Diocetyl Sebacate
KTpCIPB	Potassium Tetrakis(4-chlorophenyl)borate
PVC	Poly Vinyl Chloride
TRIS	Tris(hydroxymethyl)amino-methane
OS	Operative System
ISA	Ionic Strength Adjustor
SFTP	Secure File Transfer Protocol





Index

RESUM	I
RESUMEN	II
ABSTRACT	III
ACKNOWLEDGEMENTS	IV
GLOSSARY	V
1. PREFACE	1
1.1. Current environmental situation: heavy metal pollution	1
1.2. Origin of the present work.....	2
1.3. Motivation.....	2
1.4. Previous requirements.....	2
2. INTRODUCTION	5
2.1. Goal	5
2.2. Scope	5
3. STATE OF THE ART	7
3.1. Potentiometric detectors.....	7
3.2. Electronic Tongue	9
3.3. Artificial Neural Network	10
3.4. Flow Injection Analysis.....	10
3.5. Sequential Injection Analysis	11
3.6. Biosorption.....	12
3.7. NIVA Risk Assessment Database.....	13
4. DESCRIPTION OF THE PRESENT EXPERIMENT	17
4.1. SIA equipment description	17
4.1.1. Burette and valves.....	18
4.1.2. Control software: virtual instruments and scripts	19
4.1.3. Data acquisition	20
5. EXPERIMENTS TESTED	22
5.1. Acceptance criteria	22

5.2.	Copper electrode calibration.....	23
5.2.1.	Copper ISE external calibration	23
5.2.2.	Copper ISE internal calibration	25
5.2.3.	Tests with Copper dilutions	25
5.3.	Cadmium electrode calibration.....	27
5.3.1.	Cadmium ISE external calibration.....	27
5.3.2.	Cadmium ISE internal calibration	27
5.3.3.	Tests with Cadmium dilutions	28
5.3.4.	Cadmium calibration without cleaning	28
5.4.	Construction of cesium ion selective electrode.....	29
5.4.1.	Construction.....	29
5.4.2.	Conditioning.....	32
5.5.	Cesium electrodes calibration	33
5.5.1.	Cesium ISEs external calibration.....	33
5.5.2.	Cesium ISEs internal calibration.....	33
5.6.	Monitoring of the cesium biosorption process.....	35
5.6.1.	Grape stalk preparation	35
5.6.2.	Column preparation.....	36
5.6.3.	Calibration	37
5.6.4.	Biosorption process	38
5.6.5.	Desorption process	39
5.7.	Equipment optimisation	40
5.7.1.	Equipment set up.....	40
5.7.2.	Acquisition channels testing	42
5.7.3.	Noise reduction.....	43
5.7.4.	Complexes formation control.....	44
5.7.5.	Repeatability	45
5.7.6.	SIA software correction	46
5.8.	Online connection.....	47
5.8.1.	Frequency.....	47
5.8.2.	Data format.....	48
5.8.3.	SFTP: Secure File Transfer Protocol	49
6.	RESULTS ANALYSIS	50
6.1.	Copper external calibration.....	50
6.2.	Copper internal calibration.....	51
6.2.1.	Copper repeatability calibration.....	54

6.2.2. Cupper dilutions repeatability.....	55
6.3. Cadmium external calibration	57
6.4. Cadmium internal calibration	58
6.4.1. Cadmium repeatability calibration.....	60
6.4.2. Cadmium dilutions repeatability.....	61
6.4.3. Cadmium calibration without cleaning.....	63
6.5. Cesium external calibration	64
6.6. Cesium internal calibration.....	66
6.7. Biosorption results	68
6.7.1. 1 st Cesium biosorption.....	68
6.7.2. 2 nd cesium biosorption	73
6.7.3. 3 rd cesium biosorption.....	74
7. ENVIRONMENTAL IMPACT ANALYSIS	76
CONCLUSIONS	77
ECONOMIC ANALYSIS	79
BIBLIOGRAPHY	83
INDEX OF FIGURES	87
INDEX OF TABLES	90
INDEX OF EQUATIONS	92
ANNEX A. SCRIPTS	94
ANNEX B. DATA CARD CHARACTERISTICS	98
ANNEX C. EQUIPMENT INFORMATION	99

1. Preface

1.1. Current environmental situation: heavy metal pollution

In the last decades, a highly relevant number of scientific articles have been published over the topic of the destruction of the environment. While traditionally the publication of these papers focused mainly in the developed western countries, the increasing publication of many other countries of the rest of the world makes evident that it is not a trend in scientific research but a first order global concern.

The variation in the research has been evolving, from initially identification of the causes of this degradation to a more recent case by case studies in search for the specific pollutants. Every year more scientific fields are contributing to research for solutions and widening the variety of themes investigated. From the 1980 decade, the main topics of publications have been slowly changing from terms like, 'influence' and 'effect' to terms like 'response', 'model', 'system' or 'data', showing a clear tendency to a more problem solving approach [1].

Terms as oceanic water, continental water, ocean currents are the main topics of several thousands of the published papers. From all the fields investigated, heavy metals have an important presence in these papers. Modern embarkations are releasing considerable amount of heavy metals to the sea, yet mining and many other industries in land are generating great amounts of these kinds of pollutants that end up in the sea, washed away by the water cycle.

Some studies have shown that the presence of these materials in the water can seriously alter the development of river and marine life. It has been revealed that heavy metals are causing alterations in the DNA [2], heavy metal bioaccumulation from the simple life forms to top predators of the food chain [3] and ocean acidification among other problems [4]. Furthermore, the accumulation of these pollutants represents a thread not only to marine life and ecosystems but also to the human being. Several studies proved direct correlations between diseases and heavy metal ingestion through different pathways and exposure mechanisms [5][6][7].

Therefore, a lot of mathematical models are being designed to understand the current global processes and to foresee and prevent ecological and biological disasters. Current efforts are focused on reducing emissions and pollution, trying to prevent the consequences of the current human activities. Additionally, many efforts are being made by environmental and governmental organisations to monitor and control the waste production by the industry. In order to achieve this purpose, many investigations are being directed to create a direct, fast an on-site monitoring system.

Subsequently, in the last decades, the development of new technologies such as new sensors and on-line connectivity has created new possibilities in environmental control and protection.

Ion Selective Electrodes (ISE) have been used recently as a highly sensitive and selective system for heavy metals detection. In the present work, the calibration and optimization of a system composed by different ISEs combined with Sequential Injection Analysis (SIA) equipment. Additionally, the preparation of the developed system for online connection and real-time monitoring of the values is intended.

1.2. Origin of the present work

This Master Thesis is encompassed in the research project *“Síntesis Verde de Nanopartículas Metálicas a partir de Aguas Ácidas de Mina y Extractos de Residuos Alimentarios”* (Green Synthesis of metal nanoparticles from acid mine drainage and extracts of agrofood wastes) funded by the *“Ministerio de Economía y Competitividad de España”* (Spain Economy and Competitiveness Ministry) and by the fundraise FEDER, EU, 2016-2108 (project CTM2015-68859-C2-2-R; MINECO/FEDER).

This project is a continuation of the implementation and optimisation of the SIA system for Electronic Tongues calibration, developed in the Chemical Engineering department of the *“Escola d’Enginyeria de Barcelona Est”* (EEBE) university, in the *“Universitat Politècnica de Catalunya”* (UPC), within the Separation Techniques and Industrial Wastes Treatment research group.

1.3. Motivation

The motivation of this work is to develop an automated system for Electronic Tongues calibration for different heavy metals. Additionally, an improvement of the present invention for on-line real-time monitoring of the data obtained is intended.

The implementation of these emerging techniques in a future compact portable set in the coastal line and river basins would allow continuous monitoring of heavy metals concentration in real-time, in-line or on-line basis. This would permit a rapid response to detect gradual pollution or control in the case of environmental disasters.

1.4. Previous requirements

The previous requirements for developing this project were a basic knowledge of electrochemistry: the functioning of an electrode, the Nernst law, the basics of electricity and electrolysis process. Also,

laboratory experience in solution preparation, basic computer skills and capability to self-organise are desired qualities.

2. Introduction

In this work, a system of different Ion Selective Electrodes (ISE) combined with a Sequential Injection Analysis is tested. Previous works showed great potential of using ISEs to determine heavy metals concentrations [8]–[10]. This system was developed in previous works first with a computer controlled Flow Injection Analysis (FIA) system for metal-biosorption processes. Latterly, the ISE were implanted with a Sequential Injection Analysis (SIA) system and results were checked with UV-Visible spectroscopy [11]. Finally, the fluid dynamics of the SIA system were studied and optimised [12], [13].

In this work, the SIA system is tested, calibrated and optimised to improve the quality of the signal and reduce the electrical noise. Additionally, it is intended to add an online communication for real-time data transfer for its posterior analysis.

SIA-ISE system is calibrated by measuring the potential of solutions with different heavy metals patterns. Secondly, internal dissolutions are prepared with the SIA burette and measured inside the equipment to contrast with the ones prepared externally. Third, cesium ISEs are build following previous works procedures [14], [15] and are calibrated. Finally, biosorption and desorption process is carried out with a cesium solution in grape stalk waste and the Cs in the aqueous phase is analysed by ISE.

2.1. Goal

The aim of this project is to calibrate and optimise the SIA-ISE system, improving signal quality and reducing noise. The aim is to be able to calibrate sensors within the SIA system, to automate the SIA-ISE equipment for solutions self-preparation. Additionally, the improvement of the invention for online real-time signal transmission.

2.2. Scope

The scope of this project involves the study of the functioning of the equipment and the data acquisition program, solution preparation and equipment calibration with two different heavy metals. Biosorption is tested with cesium within the system. Also is included the research for different pathways for data transmission for online real-time monitoring.

3. State of the art

Some of the conventional analytical methods traditionally used for heavy metals concentration determination are Flame Atomic Absorption Spectroscopy (FAAS)[16] and Inductively Coupled Plasma Optical Emission Spectrometry (ICP-OES)[17]. These techniques are time consuming and require of complex equipment located in the laboratory. The limitations of these techniques have led to the search for alternatives adaptable to the study of more complex situations such as on-site, real-time determination or multimetal mixtures analysis.

3.1. Potentiometric detectors

In the context described above, potentiometric electrodes have been used in research as a feasible solution for its high sensitivity[18], good selectivity[19] and its fast response to metal ions influence. Their principle to detect the concentration of a solute in a solution is the potentiometry, which can be applied to determination of several heavy metals concentration [20].

In potentiometry, the potential between two electrodes is measured using a high impedance voltmeter to ensure that current flow is negligible. Since there is no net current, the system is in equilibrium and will react to the smallest variations of the current caused by the ions present in the solution. This technology has a very low Limit of Detection (LOD), which is in favour of the detection of heavy metal at trace level.

The set is composed by a reference electrode, whose potential is constant, and the determination electrode. When the electrodes set is placed into a solution, the variation of the potential will be detected by the test electrode in comparison with the reference electrode. The electrode system is designed so that the concentration of species of interest is the variable and all other concentrations are constant. As the test electrode is doped with ionophore for a specific metal, the selectivity will be higher for that element than for the rest of metals, giving thus an Ion Selective Electrode (ISE) [21].

The potential signals are then treated with Nernst equation. For a given standard potential, cell potential can be calculated according to Eq. 3.1

$$E_{cell} = E_{cell}^{\circ} - \frac{RT}{z_i F} \ln(a_i) \quad \text{Eq. 3.1}$$

Where E_{cell} (mV) is the potential of the cell, E_{cell}° (mV) is the standard potential of the cell, R is the gas constant, T represents the temperature (K) and F is the Faradays constant and equal to 96500 C/mol.

Z_i is the number of electrons transferred in the cell reaction and a_i is the chemical activity of the target species.

Once a potentiometry value is obtained, Nernst equation can be used to find the concentration of the sample solution. If temperature is considered constant at 298 K, the equation can be simplified. Furthermore, the z_i coefficient is constant for a specific metal, leaving the equation as presented in Eq. 3.2.

$$E_{cell} = E_{cell}^{\circ} + s \times \log (a_i) \quad \text{Eq. 3.2}$$

From this, the activity coefficient is a non-constant number of a specific chemical species that is determined by the activity coefficient (γ) multiplied by the concentration.

$$a_i = \gamma \times c \quad \text{Eq. 3.3}$$

Since γ tends to the unity at low concentrations, activities in the Nernst equation are frequently replaced by simple concentrations (Eq. 3.4).

$$E_{cell} = E_{cell}^{\circ} + s \times \log (c) \quad \text{Eq. 3.4}$$

The theoretical result of the calibration can be obtained from Eq. 3.4. By using the number of electrons of the specific metal in the equation coefficients (n), a 1st grade equation is obtained:

$$E_{cell} = K + \frac{59.16}{n} \times \log (c) \quad \text{Eq. 3.5}$$

Where K is a constant, the independent variable is the solution concentration and the theoretical slope to be obtained depends on the metal determined. In case of copper and cadmium, n is equal to 2 and the resulting equation is **¡Error! No se encuentra el origen de la referencia.**Eq. 3.6.

$$E_{cell} = K + 29,58 \times \log (c) \quad \text{Eq. 3.6}$$

When other metals such cesium are being analysed, the value of n can differ. In the case of cesium, its valence is different from the two previous metals.

$$E_{cell} = K + \frac{59.16}{1} \times \log (c) \quad \text{Eq. 3.7}$$

$$E_{cell} = K + 59,16 \times \log (c) \quad \text{Eq. 3.8}$$

Where K is a constant, the independent variable is the solution concentration and the theoretical slope to be obtained is equal to 59,16 (Eq. 3.8).

3.2. Electronic Tongue

Although ISE have been known for a long time and more than 50 analytes are known, their practical use was minimal. Their LOD was not low enough and usually reached only 10^{-4} molar concentrations. Nevertheless, significant improvements have been made in the past few years. Current ISEs of many analytes are capable of detecting 10^{-6} , 10^{-8} and even 10^{-10} molar concentrations, which is lower than parts per billion levels. This renewed the interest in this technology and many researches are now exploring the potential of the ISEs [22].

Nowadays in some new technologies under development, mimetic the nature is a key concept to achieve what is already produced chemically or biologically in the nature. Last ISEs papers show a clear tendency of putting together different sensors to achieve a multimetal detection [9]. An array of ISEs can interact and detect selectively different metals within a single solution. This capacity is usually compared with the capability of the tongue to detect different substances or 'tastes' in a mixture of compounds. For this reason, sensors arrays composed by different metal sensitive ISEs are usually described as Electronic Tongue (ET) in the literature[23].

The potential utility of an ET is very wide [24]. Its low LOD and the possibility to add as many electrodes as needed makes this technology a high potential tool for continuous real-time analysis. Combination of sensor array and automated system of pumps and valves, governed by virtual instruments proved to be very useful for copper biosorption process monitoring [8], [9] compared with the results obtained by FAAS and ICP-OES. The use of virtual instruments allowed to program self-calibrating system and to detect with a high accuracy the metal concentration. This allowed modelling a breakthrough curves by Thomas model for the sorption of Cu (II).

The optimisation of the ET permitted the creation of a 9 sensors array for different heavy metals detection at the same time. Real-time monitoring of different binary and ternary mixtures was achieved. All sensors showed certain cross response to the target ions. Interference between ISE and the metals non targeted present in the solution can be determined by the fixed interference method (FIM). The FIM method implies using test solutions with a constant interfering ion concentration while the primary ion concentration is varied [25]. As a mathematical method of data processing an Artificial Neural Network (ANN) is used (see next section).

The great advantage of the ET is the possibility of miniaturisation of the different ISEs used in the tongue. The analysis with ET allows determining a great variety of species with a reduced sample

volume. According the literature reviewed: “It has been demonstrated that electronic tongues are an appropriate tool for simultaneous measurements in the monitoring of flow processes” [8].

3.3. Artificial Neural Network

When characterizing a combination of ISE, the Nernstian responses for the corresponding primary ion are obtained. Nevertheless, the cross-response of the ISEs to non primary ions is an important feature when modeling the behaviour of an ET. It is unavoidable that ISEs show certain degree of affinity to target ions, yet this is a desirable situation for building an ET. This interaction can be identified and taken into account for defining a better model of response. For that, an Artificial Neural Network can be used [8].

ANN are computer systems that have certain similitude to biological neural networks, on which they are based. Such systems learn how to perform tasks through experience, without any previous knowledge. They automatically generate identifying characteristics from the learning material that they process. Once an ANN has been trained, it can perform, for example, a determination of ion concentration, by taking into account the multiple interactions between the various species present in a solution and the different ISEs lectures of the same sample. In the recent literature [8] an ET with an ANN was trained with binary mixtures of Cu^{2+} and Pb^{2+} , Cu^{2+} and Zn^{2+} , and ternary mixtures of Cu^{2+} , Pb^{2+} and Zn^{2+} and Cu^{2+} , Pb^{2+} and Cd^{2+} .

With the selection of the appropriate parameters for data processing, the utility of an ANN for ET signal processing is postulated as a very good option with a high potential.

3.4. Flow Injection Analysis

Many analytical techniques require a concrete volume, carefully selected and transferred, for chemical determinations [26], [27]. These techniques, defined as Flow Injection Analysis (FIA), are used for fast determination with low signal noise and high signal quality.

FIA was the first flow technique developed in 1975 and it has been widely used in analytic techniques such as spectrophotometry and potentiometry. A FIA system (Figure 3.1) is composed by the carrier solution, which is transferred thanks to a peristaltic pump, generating a constant flow of carrier to the detection system. Secondly, an injection valve allows to introduce samples without interrupting the general flow to the detector. A reaction loop is needed in order to store the solution previous to the analysis. Finally, a detector analyses the flow giving a continuous real-time monitoring.

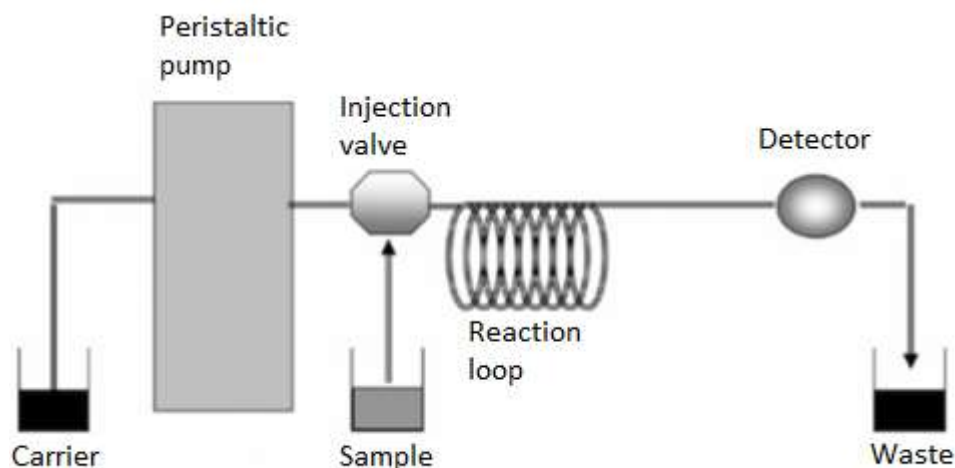


Figure 3.1 Standard FIA system [27].

3.5. Sequential Injection Analysis

The Sequential Injection Analysis (SIA) was intended to represent the next step in the FIA systems, adding certain improvements related to system simplification and savings in reagent usage. Nevertheless, the different possibilities of each technique have made them complementary. The high costs of maintenance of the peristaltic pump and the need of rearrangement all the FIA system for each experiment tested lead to the creation of the SIA configuration. The sequential injection allows saving reagents and samples by not providing a continuous flow to the detectors. One of the difficulties of the SIA implementation has been the need to configure a computer to control all the instrumentation plus the software necessary for that task.

Because of the industrial pollution of the river waters, European requirements of water pollution have become more restrictive. This fact has made the monitoring of water a matter of importance. In this context, the versatility that offers SIA places this technology as one of the most important for water monitoring, as the literature demonstrates [28].

A SIA system (Figure 3.2) is based in the same principles than FIA, but composed by an automated burette that promotes a laminar flow, plus giving the opportunity of reversing the sense of the flow. This system allows controlling the inlet of different reagents to create multiple solutions. Taking this fact into consideration, different solutions can be used together to calibrate a system easily. Carrier and mono-elemental pattern solutions can be mixed to produce multi-elemental pattern solutions which can be time-saving to train the ET.

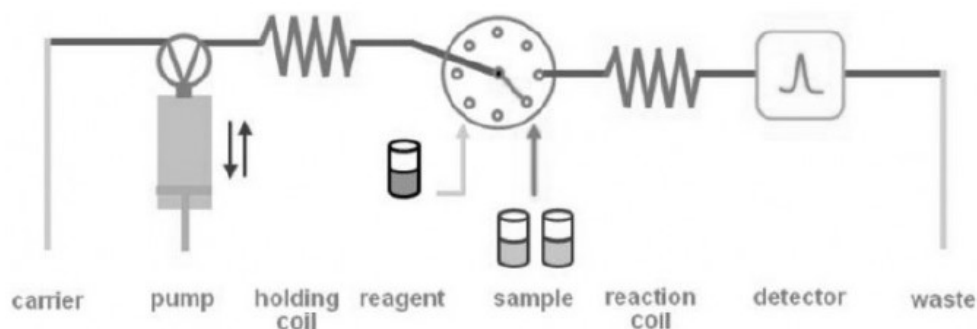


Figure 3.2 Standard SIA system [29].

The optimisation of these methods will allow creating multimetal detectors. The detectors based in ISE arrays have the advantage that they can be reduced to a portable device. The potential of this technology permits monitoring water environments such coastal line and river basins with a lot of elements dissolved. The volume of data generated in the next decades is expected to increase.

The possibility of real-time monitoring generates the need of processing the data simultaneously. This will give a head start when solving environmental issues, preventing natural disaster or industrial accidents. Therefore, the maturation of these technologies will have to be followed by an improvement of data treatment in real time. In this work, connection of the present invention with risk assessment database is considered.

3.6. Biosorption

Among many techniques studied for heavy metal removal from water [30], biosorption is one of the most cost-effective techniques researched [31]. Biosorption has been deeply researched in the last two decades due to its great capacity for absorbing different pollutants and even bioremediation has been used in the recent past for minimizing the impact of natural disasters [32]. Heavy metals biosorption has been proved as “a promising technology for removal of heavy metals from aqueous solutions” [33] due to its low cost and high efficiency.

Some researched techniques required preliminary chemical treatment in order to achieve certain degree of biosorption onto biomass [34]. Nonetheless, other approach of the investigation has been focused on reusing agricultural wastes directly for metal absorption without any additional costs [35], [36].

In this context, grape stalk wastes are produced by the wine industry in the Mediterranean area in great amounts. Different studies have used it to test and analyse its capacity for absorbing different

heavy metals [37], [38]. Through a ion exchange mechanism, grape stalk waste proved its capacity as a biosorbent for different heavy metals [39], [40] and its kinetics were determined [14].

In the present work, biosorption was tested within the SIA system in order to monitor the biosorption through the equipment.

3.7. NIVA Risk Assessment Database

The analytical techniques traditionally used for determining the level of pollutants usually require of complex equipment placed in the laboratory and are not suitable for on-site analysis. The use of the ISE's system above described allows determining the concentration of heavy metals at real time. This, combined with the feasible reduction and optimization of the equipment for an on-site device, introduces the possibility of online monitoring of heavy metals concentration.

The use of sensors with online connection for environmental monitoring has been increasing exponentially during the last two decades. The increasing volume of data gathered by the control centres has created the necessity of real time evaluation of the results in order to give a rapid response to the threads towards the environment.

The data processing has been traditionally faced in a case-by-case manner. The processing of data has become highly cumbersome and time-consuming. The possibility of processing large number of data in a short time and with high quality assessment remains unchallenged. There is a need of solving this issue by reducing the processing time and the uncertainty of the results [41].

For all the online monitoring systems and for emerging technologies such as the one described in the present work, the Norwegian Institute for Water Research (NIVA from now on onwards) has developed a Risk Assessment Database (RAdb). It is a tool that that facilitates rapid and consistent hazard and risk assessment of single chemicals and mixtures of these.

The NIVA RAdb is a module-based tool that compiles, organizes and integrates the available information of exposure and effect in order to accelerate the assessment for a given situation and pollutant involved.

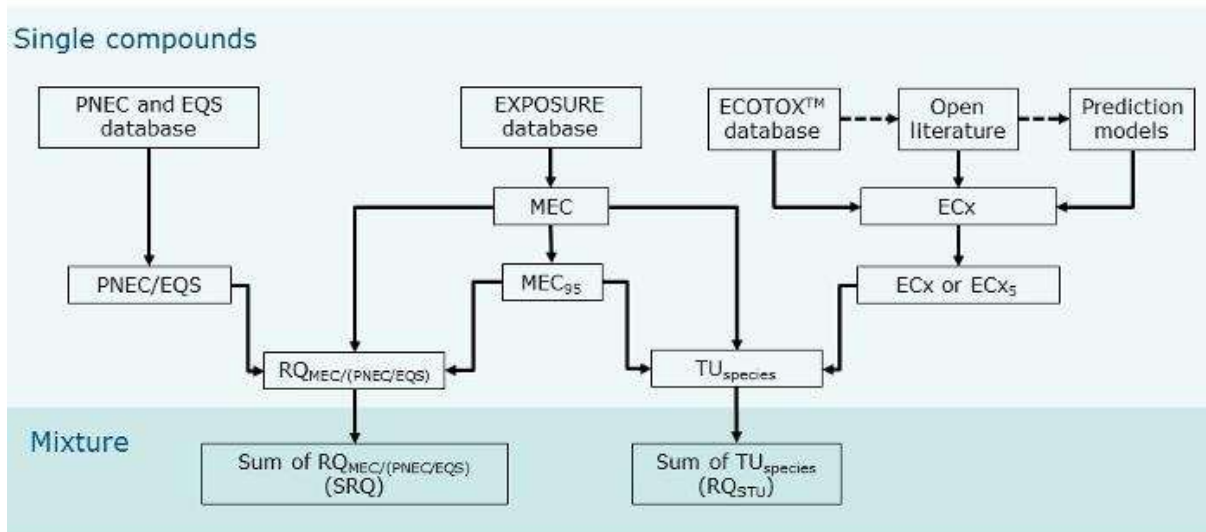


Figure 3.3 Overview of NIVA RAdB operating mechanism [41].

In the Figure 3.3 an overview of NIVA RAdB is shown. The operating mechanisms are described by NIVA as: “were data compilation, integration and calculations are performed on exposure and effect data. Exposure data is provided as Measured Environmental Concentrations (MEC) and 95% percentile of the MECs (MEC₉₅) are calculated as a “worst-case” exposure scenario in cases where sufficient data are available. Effect data is compiled as Predicted No Effect Concentrations (PNEC) and Environmental Quality Standards (EQS) or as Effect Concentrations (EC) for a given toxic effect x (ECx). The ECx values are obtained from the ECOTOX (™) database or open literature, and complemented by predicted data generated by Quantitative Structure Activity Relationship (QSAR) models when experimental data was not available. The 5% percentile of the ECs (ECx₅) from single species data is calculated as a representative of the “most sensitive” species within a species-group (e.g. algae, crustaceans, fish and amphibians). The resulting exposure and effect data are used to calculate a risk quotient (RQ) based on PNEC/EQS data (RQ_{MEC/(PNEC/EQS)}) and a species group-specific RQ based on Toxicity Units (TU_{species}) as a risk prediction of single compounds. Summation of the RQs is performed as a prediction of the cumulative risk of mixtures assuming principles of Concentration Addition” [41].

The benefit of data compilation lies in the hierarchical comparison of the detected levels to the literature. This allows determining if a certain chemical is related to a molecular target, causing a cellular response, if the cellular damage can affect an organ and thus can influence on the individual or even the population of the studied organism. The result of the analysis will help defining the Mode of Action (MOA) of one or more chemical compounds. The NIVA RAdB can help find risk drivers such as the most toxic chemicals and susceptible species by calculating risk quotients.

The NIVA RAdb can be a great tool for real time monitoring but also can help finding new relations between chemical stressors and final outcome effects on the individual through the metadata generated. If any new and existing research is included from in vitro bioassays to whole organism bioassays and field studies, the database can be of great use for water environments risk assessment. Furthermore, the continuous development of this technology should allow it to expand to terrestrial environments.

The interest of the NIVA RAdb for the present work is that processing pipeline to import data from remote elements into NIVAs Risk Assessment database (RAdb) for real-time and automated monitoring of the Hazard and Risk of metals has been developed. Data can be automatically transferred as output files from the chemical sensors to a SFTP server at NIVA by internet. The imported data can be then processed in the NIVA RAdb for subsequent calculation of Hazard (HQ) and Risk quotients (RQ) based on available information managed in the database. Future development will display the HQ and RQ and highlight the values above the threshold.

4. Description of the present experiment

4.1. SIA equipment description

According to the principles described in the previous section, the equipment was set in the previous works to be used as a SIA (Figure 4.2). The equipment is divided in three main parts: the burette (left), the main body (centre) and the control computer (right). Both burette and equipment are connected to the computer but not between them. Control of all the operations only occurs from the computer.

The main body is composed by the retention coil, where 7,64 meters of conduit are winded around a cylinder. This creates the possibility of holding more volume of liquid inside the equipment and therefore being able to perform longer essays within a single movement of the burette. The retention coil is followed by the channels for the reagents input, where solutions of different concentrations can be introduced in the SIA system. The mixing cell is only used when creating solutions internally by mixing different solutions or a solution with the carrier. Finally, the acquisition channels are the ports for the ISEs connection.

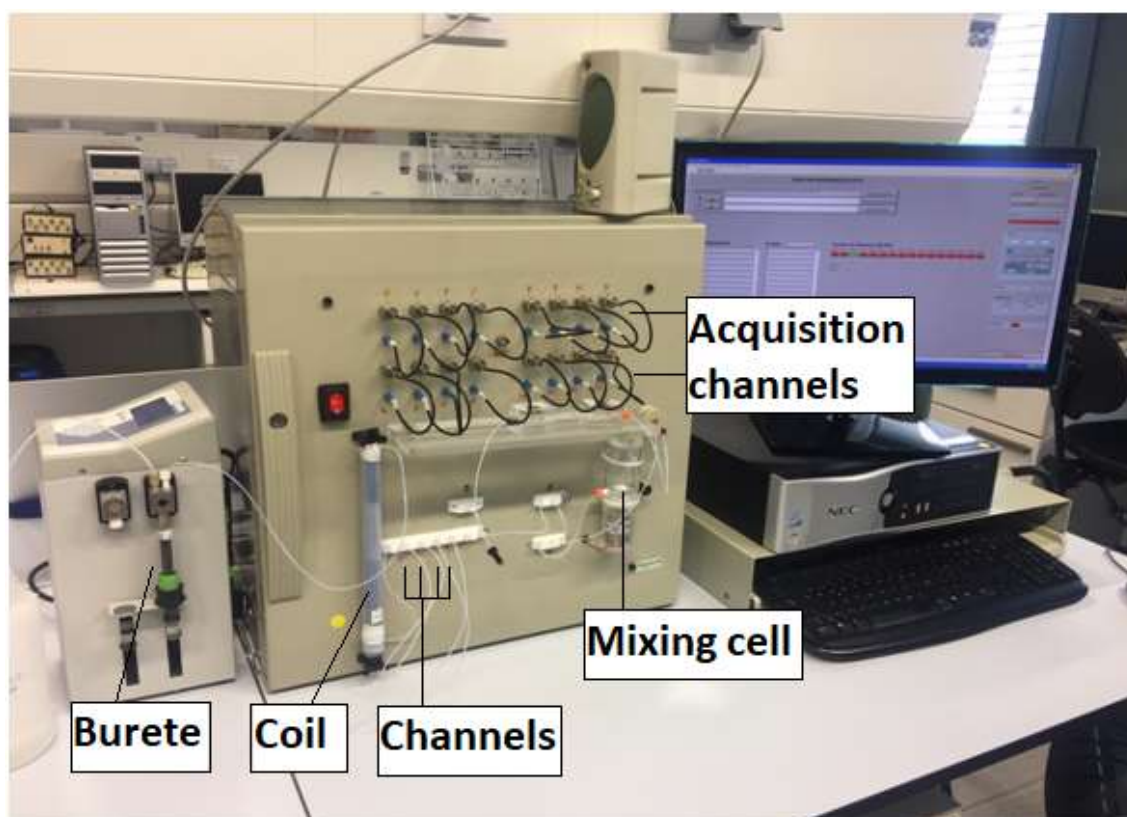


Figure 4.1 SIA system in the EEBE laboratory [42].

Figure 4.2 shows a diagram of the internal SIA conducts. In the next pages, the set up and functioning of the equipment is described.

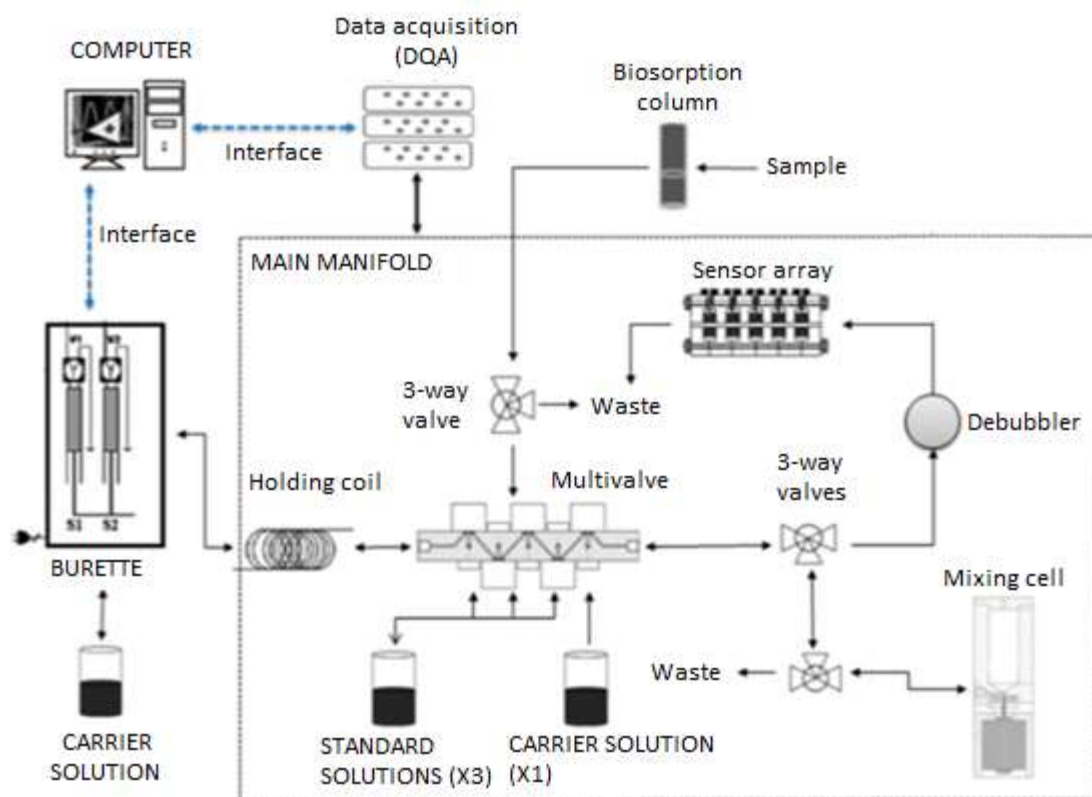


Figure 4.2 SIA system diagram [12].

4.1.1. Burette and valves

The vertical movement of the burettes is used to push forwards and backwards the carrier solution depending on its direction of movement (Figure 4.2). Its importance lies on the possibility of creating different solutions within the system without needing any modification of the latter one. The main body is composed by several conductions and valves that create the SIA. The burette movement can transfer in/out a maximum volume of 5 ml. From the burette, there is a 'main path' that goes straight to the electrodes. Through the way, different elements are conduit to the main path and their entrance is regulated by valves. The 3 way valve from the left controls whether the solution from the absorption is sent to the detectors or wasted. Finally the other 3 way valves control when the solutions to be analysed are sent to the sensors array or they are loaded to the mixing cell for creating different concentrations solution in an automated way.

The insertion of sample aliquots and reagents is controlled by the multivalve operation. Figure 4.3 shows an example of samples operation. After filling the burette with carrier (a) and cleaning the

system (b), reagent is collected (c), followed by sample collection (d) and more reagent (e). Later, by operating the burette, the liquids could be combined in a mixing cell for latterly sending it to the sensors for its analysis (g). This kind of operation is very usual and simple with the SIA equipment, allowing performing several experiments in a short time and with a few standard solutions.

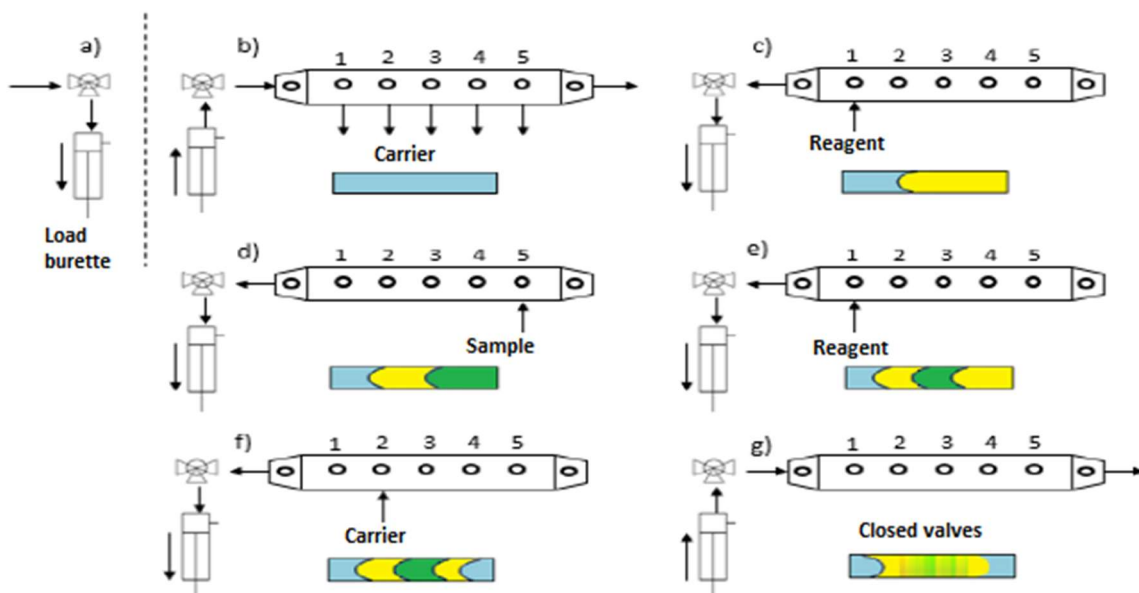


Figure 4.3 Example of dilution with the diluent through reagent channels [12].

Blue: Carrier; Yellow: Reagent; Green: Sample;

4.1.2. Control software: virtual instruments and scripts

The equipment is controlled from the computer by the software Labview, from National Instruments®. A specific program was created for controlling this equipment in previous works[12]. It is composed by diverse virtual instruments that can receive the orders from the computer to execute commands in specific parts of the equipment. Virtual instrumentation is a clear trend with computer-based measurement systems.

The advantage of working with Labview is the possibility of modification the commands in a simple manner and without having to modify the main software. By programming scripts in a .txt format, operations can easily be written. Some of the most used commands included burette motion, valve operation, to turn on/off data acquisition, to introduce waiting time or to turn on/off the mixing cell stirrer. The most important scripts used during the realisation of this work can be found in the annex A.

More than one script could be queued in a list in order to let the equipment performing several experiments without the need of the operator control. To do so, the scripts could be listed in an 'experiment' and they consisted in .txt files that called the different scripts to be performed.

4.1.3. Data acquisition

The ISEs in contact with solutions are permanently giving potentiometry lecture. Data acquisition is design to take advantage of this by recording values periodically. The frequency of data recording can be defined by modifying the software of the program and, in the present work, it was established in 0.1 seconds.

The data values are generated by the electrodes and recorded by a data card. The data card used (see annexe B) has the capacity of generating 250.000 values per second. Since the purpose of the experiments is the monitoring of long-lasting heavy metals tests, the volume of data generated is much larger than needed. The data treatment of that amount of data points would increase the time for data processing exponentially. Therefore, the software is programmed to reduce it by the next mechanism.

The Labview software is programmed to register 1000 values and record each of them every 10.000 Hz. This means that the equipment will be 'reading' 1 value every 10^{-5} seconds until 1.000 values are 'read' and the average is calculated. Therefore, every 0.1 seconds, the program will record a data point, which is backed up on 1000 measurements, performed during that period.

$$\frac{1 \text{ value}}{10.000 \text{ Hz}} \times 1.000 \text{ values} = 0.1 \text{ seconds} \quad \text{Eq. 4.1}$$

The frequency of the data acquisition and the number of values averaged for each data line recorded can be modified. Different tests were performed to optimise this parameter. First tests were attempted with more values to be averaged, in order to increase the robustness of the results. These experiments resulted in errors in the time that the equipment needed to perform the experiments. That happened due to the high amount of values to be checked which required more time for the system to do the data treatment. Therefore, with the established frequency (10 kHz), no more than 1.000 values were averaged.

Later, tests were executed with less values to be averaged (i.e. 500) and the system could perform without any conflict. The experimental time was not elongated by the data acquisition and the system worked at the expected rate. The inconvenient of using this frequency was that the noise of the signal slightly increased. Since the program could work with a higher number of values to be averaged per line recorded, the noise was chosen to be avoided as maximum as possible and hence,

5. Experiments tested

The mode of action followed is composed by three steps: external calibration of the electrode with specific heavy metal solutions in a pH-meter (see annexe C), internal calibration with the electrodes connected to the SIA equipment and finally by the determination tests. In the last stage of the project, an ISE was built in the laboratory, calibrated and tested by doing a biosorption study. The experiments tested are described in the next pages.

5.1. Acceptance criteria

In order to evaluate the results obtained in the experiments, certain previous requirements were defined. The goal was to discriminate between good and bad results objectively and hence, to identify any tendency, shift or irregularity in the results.

The requirements previously defined were as stated below:

Table 5.1 Acceptance criteria.

Coefficient	Acceptance criteria
Linearity	$0.990 < x$
Margin of error – Slope*	10 %
Solutions stability**	$X < 0,5 \text{ mV / min}$

**The margin of error of the experimental slope in front of the experimental slope is wide. The slope of the calibration is considered only qualitatively. The similitude between the theoretical and experimental slopes is an indication that the electrode has selectivity for the target ion and that the solutions are well prepared. See page 50 and beyond for more detailed description of the calibrations.*

***Before starting any external calibration, the electrodes were immersed in the carrier solution and waited until the potential detected was constant. The acceptance criteria for considering the potential as constant was that the potential variation during a minute was less than $\pm 0,5 \text{ mV}$.*

In the internal calibrations the stability is considered differently. When the solutions have reached their maximum potential value and the signal is not varying, the stability would be the capacity of the electrodes to detect the same value continuously.

5.2. Copper electrode calibration

A copper ion selective electrode was tested in the first place. Previous works and own experiences in the laboratory suggested that copper ISE would have a good and a high selectivity. The commercial ISE for copper (II) ions from Thermo was used (see annexe C). As a reference electrode, a double junction electrode from Thermo was used for all the tests performed in this work. The reference electrode was composed by potassium chloride (KCl) as electrolyte and potassium nitrate (KNO_3) in the outer chamber to guarantee an ionic medium.

For the calibrations, standard solutions of copper nitrate ($\text{Cu}(\text{NO}_3)_2$) were prepared (Table 5.2). Concentrations of the solutions prepared were designed to cover the expected lineal range of the electrode.

Table 5.2 $\text{Cu}(\text{NO}_3)_2$ standard solutions.

Concentration	10^{-1} M	10^{-2} M	10^{-3} M	10^{-4} M	10^{-5} M
Volume	100 ml	100 ml	100 ml	100 ml	100 ml

$\text{Cu}(\text{NO}_3)_2$ was weighted in an analytical balance (see annexe C) and flushed with ultrapure water. The solution used as a Ionic Strength Adjustor (ISA) was composed of KNO_3 . Equally to the standard solutions, potassium nitrate was weighted in the analytical balance and flushed with ultrapure water to a concentration of 10^{-1} M.

5.2.1. Copper ISE external calibration

The copper ISE was placed in a support along with the reference electrode and both together were immersed in the solution (Figure 5.1). External calibration was performed only in the lower range of concentrations. First, 20 ml of potassium nitrate were added into the glass baker. pH-meter was configured to measure the potential in mV and then the electrodes were immersed and acquisition program was initiated.

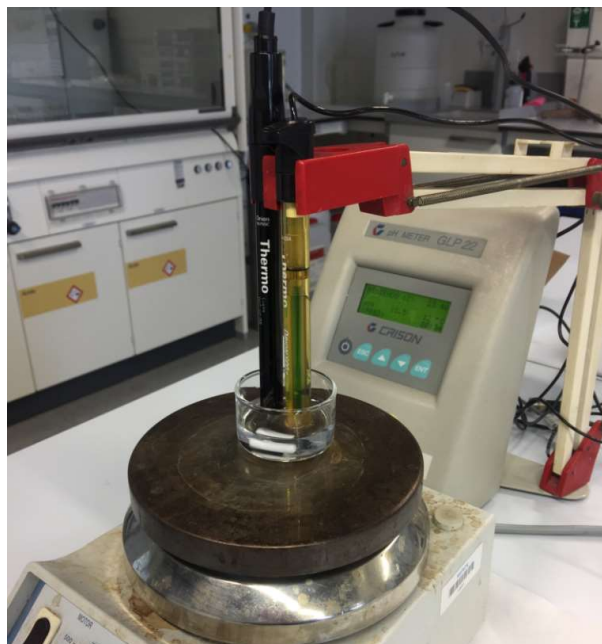


Figure 5.1 External calibration [42].

The calibration was only started until the value of potential obtained from the carrier solution was stable.

When the limit was accomplished, the solution and the electrodes were considered steady and the additions were performed. The volumes added and the concentrations are shown in the (Table 5.3).

Table 5.3 Copper external calibration.

Concentration added (M)	Volume added (μ l)	Total Volume (ml)	Concentration (M)	log C
0	0	20	0	-7
0,001	25	20,025	1,25E-06	-5,9036
0,001	50	20,075	3,74E-06	-5,4276
0,001	100	20,175	8,67E-06	-5,0618
0,001	250	20,425	2,08E-05	-4,6818
0,001	500	20,925	4,42E-05	-4,3545
0,01	100	21,025	9,16E-05	-4,0383
0,01	250	21,275	2,08E-04	-3,6820
0,01	500	21,775	4,33E-04	-3,3637
0,1	100	21,875	8,88E-04	-3,0516
0,1	250	22,125	2,01E-03	-2,6973
0,1	500	22,625	4,17E-03	-2,3795

The progressive increases of the concentration and the potential increase detected by the electrode were recorded. The linearity and the slope could be successfully calculated (page 50).

Many calibrations were made during the realisation of this project. All the observations made and the changes applied in order to improve the equipment performance are described from page 40.

5.2.2. Copper ISE internal calibration

After the successful external calibration, the copper ISE was tested in the SIA equipment. The solutions used were the same as the ones used in the external calibration: KNO_3 as carrier and $\text{Cu}(\text{NO}_3)_2$ as the metal ionic solution. This allowed comparing the values obtained to the ones in the external calibration.

The reference electrode and the copper ISE were placed in the PMMA supports as explained in the section 5.7.1. The carrier solution was introduced in the system by the burette and it was pushed to the retention coil and the electrodes (see Figure 4.2) to fill the conduits, eliminating the air of the system. Depending on the position of the valves, the solution introduced in the system is moved from the carrier solution or from one of the channels. The same occurs when emptying the burette. As the burette was closing, the solution or sample was expelled to the retention coil and the electrodes.

Secondly, the lowest concentration copper solution (10^{-5} M) was introduced in the system through the reagent channel 1. In order to do that, the burette introduces the solution into de SIA by inverting its movement. The sample to analyse, which in this case is the solution, was carried to the retention coil. Finally, the burette moves the copper solution towards the electrodes.

The volumes transferred during internal calibrations were designed in a way that at the end of the solution detection, no more sample was left in the tubing and carrier solution was already being measured. With this, a system cleaning procedure was performed. Additionally, four full burette movements (4 x 5 ml) filled with carrier solution were transferred through the system between different samples detection to make sure that there was no previous solution left.

These stages were repeated for every solution in an increasing concentration order, followed by the opposite order. This means from 10^{-5} M to 10^{-2} M and, again, from 10^{-2} M to 10^{-5} M. The goal was to check if the system had hysteresis. All the data were recorded by the SIA equipment and displayed graphically by the Labview software, with the potential in mV in the Y axis and time in seconds in the X axis.

5.2.3. Tests with Copper dilutions

After successful calibrations were performed, a series of internal dilutions were prepared inside the equipment with the mixing cell. The goal was to be able of creating any dilution internally for future ET calibrations. In order to do that, the dilutions were compared to the calibration curves obtained to

check if the potential value obtained experimentally matched with the ones calculated with the curve.

Dilutions were prepared by mixing different ratios of a standard solution with carrier solution. The operation was performed in two different ways:

- a) By sending both the standard solution and the carrier through reagent channel (Figure 4.4).
- b) By sending the carrier through the burette, as done when performing calibration.

Both methodologies are based in the volume that is being introduced in the mixing cell by calculating the volume of fluid being transferred through the conduits.

Method a) was designed in previous works [13] and tested successfully. This method was tested for copper solutions in the present work. A single dilution was made within the SIA equipment and measured in the electrodes. In order to evaluate if the dilution was successful, the potential value obtained was compared to the expected potential from a 10^{-3} M solution. To evaluate this, the calibration curve obtained that day of experiment was used:

$$Y = 30,7 \times X + 198,7 \quad \text{Eq. 5.1}$$

Therefore, for a potential (Y) of 106 mV obtained, the expected concentration (10^X) is obtained. The concentration of the dilution was $9,55 \cdot 10^{-4}$. This result has a margin of error (MOE) of 4,5 %, therefore the dilution was very exact.

Method b) was used in the subsequent tests. The mode of action of this method is that the standard solution to dilute is introduced from one of the reagent channels and the carrier solution is introduced directly from the carrier reservoir, in the other conduit that leads to the burette (see Figure 3.2). There are two main advantages of operating like this. First, that the carrier solution is not introduced through a reagent channel. This leaves one conduit free to introduce one more standard solutions without having to clean and change the reagent. Secondly, the difficulty of the operation is much simpler and less reagents consuming. The burette only has to introduce standard solution through one channel to the main conduit and transport it with the carrier to the mixing cell. The only difficulty is to have the exact volume of carrier inside the mixing cell.

Dilutions were tested with the second method (b). The dilution tested was to dilute a 10^{-2} M solution to $2,5 \cdot 10^{-3}$ M with the proportional amount of carrier solution. Because of the simplicity of the second method and the lesser time elapsed, 10 dilutions were programmed consecutively. The goal was to have a more robust calculation of the MOE. Additionally, the experiment tested was used to evaluate repeatability.

5.3. Cadmium electrode calibration

After the tests performed with the copper ISE, similar experiments were repeated with the cadmium ISE. As explained for the copper, experiments usually included external calibration by using the pH-meter, internal calibration in the SIA equipment and dilution tests. Additionally, some other experiments were performed.

5.3.1. Cadmium ISE external calibration

The commercial ISE for cadmium (II) ions from Orion was used (see annexe C). As a reference electrode, the same double junction electrode was used for the cadmium tests.

The procedure followed for calibrating the cadmium ISE was the same than the one followed for the copper calibration. Standard solutions of Cadmium nitrate ($\text{Cd}(\text{NO}_3)_2$) were prepared (Table 5.2). Concentrations of the solutions prepared were designed to cover the expected linear range of the electrode.

Table 5.4 $\text{Cd}(\text{NO}_3)_2$ standard solutions

Concentration	10^{-1} M	10^{-2} M	10^{-3} M	10^{-4} M	10^{-5} M
Volume	100 ml	100 ml	100 ml	100 ml	100 ml

$\text{Cd}(\text{NO}_3)_2$ solutions were prepared with ultrapure water. The solution used as a ionic strength adjustor was composed of KNO_3 . Equally to the standard solutions, potassium nitrate was weighted in the analytical balance and flushed with ultrapure to a concentration of 10^{-1} M.

Equally to the copper solutions, external calibration was performed by immersing the cadmium ISE and the reference electrode in 20 ml of carrier solution. The calibration was started when the potential value generated by the carrier solution was stable. Later, gradual additions of cadmium solution were added, and the potential values generated were noted.

The gradual addition of cadmium standard solution was followed by a gradual increase of the potential. Calibration curve is calculated and results are analysed in page 56.

5.3.2. Cadmium ISE internal calibration

Once the cadmium electrodes were tested externally and results obtained fulfilled the acceptance criteria, internal calibration was performed. Same cadmium standard solutions were used than for the external calibration and, as a carrier solution, KNO_3 0,1 M was prepared.

In the first cadmium calibration the hysteresis test was performed, making an increasing and a decreasing calibration. This means that standard solutions were used in increasing and decreasing concentration order: from 10^{-5} M to 10^{-2} M and, again, from 10^{-2} M to 10^{-5} M.

The maximum values acquired during each solution detection were recorded (Table 6.9). These values were used to calculate the calibration curve (section 6.4). Again, two calibration curves were calculated, from the increasing and the decreasing concentration calibration respectively.

5.3.3. Tests with Cadmium dilutions

Cadmium tests were carried after all the copper tests were performed and so, the attempts of preparing internal dilutions were directly performed with the b) method described in section 5.2.3. Carrier solution was used as a diluent and introduced into the system through the burette. As performed with copper ISE, equal dilutions of cadmium were made consecutively to evaluate the repeatability of the dilution system. The curves obtained for the 8 dilutions performed are shown in the next figure. It was not possible to make 10 consecutive dilutions due to a system error in the acquisition, which was amended lately in the equipment optimisation phase (see section 5.7).

The analysis of the results and the evaluation of the performance of the dilution system is done in the section 6.4.2.

5.3.4. Cadmium calibration without cleaning

Considering the good stability obtained in the previous experiments, cadmium electrode and cadmium solutions proved to be very steady and easy to work with. Therefore, more experiments were performed with this electrode in order to use it to optimise the equipment and the experimental methodology.

A new calibration with a different approach was considered. The repeatability experiments of both heavy metals showed that the measure improved after the 4th consecutive determination. This happened because of the total volume used during those determinations. In other words, the accuracy of the method was accomplished only when sufficient volume of the solution to analyse was used and there were no previous solutions left even at trace level.

With this reasoning, it was considered that the conduits cleaning did not need to be performed exclusively with carrier solution, but it could be done with the next standard solution instead. Therefore, a calibration with no cleaning stages was designed. In order to ensure that there were no previous solution traces left, the volume of solution to analyse was increased from 5 ml to 15 ml. As the burette maximum volume is 5 ml, three consecutive movements were done for each standard

solution determination. This means that 3 x 5 ml of 10^{-5} M solution were analysed, followed by 3 x 5 ml of 10^{-4} M, 3 x 5 ml of 10^{-3} M and finally 3 x 5 ml of 10^{-2} M.

The volume used for the calibrations was 15 ml for each concentration. This volume required three burette full movements of 5 ml. In the data acquisition the values were taken as 3 individual determinations, one for each burette movement. With this, the difference between different determinations of the same solution could be identified. The results obtained are shown in the next table, written in the same order they were acquired, from the first value in the top, to the last one in the bottom.

As can be seen, no clear trend or drift is observed between the values of each concentration, even though some values decrease after repetition. Therefore, no effect was observed by the lack of cleaning. These results were used for calculating a more robust calibration curve, with three points for each concentration. See calibration results analysis in page 63.

5.4. Construction of cesium ion selective electrode

5.4.1. Construction

A third metal was tested: cesium was chosen because it is usually related to environmental problems such as radioactivity and its monitoring is of great interest. The goal was to build an ISE in the lab with a simple procedure and to use it to monitor a biosorption process of Cs onto grape stalk waste. Cesium is a well-known metal that has been deeply studied in biosorption processes[15].

The feasibility of building this kind of electrodes is very important, because it makes accessible the investigation to other laboratories without having to purchase additional equipment. Also the constructed ISEs are made with a polymeric membrane over a graphite base. This membrane can be easily applied and also removed. This allows the reutilisation of the electrode body for further uses.

In this work, four electrodes were prepared: two conventional and two tubular (Figure 5.3 and Figure 5.4). As all of them were previously used, their polymeric membrane was removed and they were polished until graphite was totally exposed. Also their conductivity was checked with a tester. The advantages of building four instead of one is that spare electrodes would be available in case of rupture or failure in the construction process. Additionally, it would be possible to compare conventional and tubular electrode configuration. The conventional electrodes were named as C1 and C2, while tubulars were defined as T1 and T2 respectively.

The reagents necessary for an electrode construction are the ionophore, which is the element that will have selectivity towards the target ion [43]. An anionic additive, which rejects anions, allowing

only cations to go through and reducing the noise detected by the electrode. A polymeric resin to mix all the components. A plasticiser, which is an organic solvent, to maintain the ionophore dissolved within the resin. The elements chosen for each of those components are based on previous works [14] and are described in the lines below.

The main body of the electrodes is built of graphite because its conductivity. This permits that the electrode transfers the signal to the wire, and then, to the equipment. The cables of the chosen electrodes were checked with a tester to control if they conducted electricity and that there were not damaged. Finally, the mixture for building the electrode was prepared.

Ionophore: The ionophore used in this work is the cesium ionophore (III), (thiacalix[4]-bis(crown-6)) with the chemical formula: $C_{44}H_{52}O_{12}S_4$.

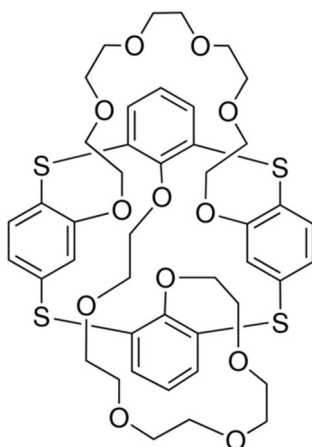


Figure 5.2 Ionophore thiacalix[4]-bis(crown-6) [43].

Plasticiser: Different plasticisers were studied by the authors of the previous studies [43] and the dioctyl sebacate (DOS) was found to be the one which offered a wider linear range.

Anionic additive: It was demonstrated that the use of additives such as KTpCIPB improved the performance of the slope obtained with the electrodes.

Polymer: The polymeric resin used as a binder was made of PVC.

Once the reagents were prepared, each of them was weighted in an analytical balance and added into a test tube with screwcap. The proportions necessary for the construction of the electrode are depicted in the next table.

Table 5.5 Mixture composition [43].

Reagent	Proportion (% w/w)	Amount of reactant
Ionophore	1	3,2 mg
Plasticiser (DOS)	66	216 μ l
Binder (PVC)	33	99,1 mg
Additive (KTpCIPB)	25	0,37 mg

Once each reagent was added, the reagents were mixed by putting the tube in an agitator (SBS mixer AT-1) for 10 seconds.

Once the mixture was prepared, 3 ml of tetrahydrofuran were added to the test tube to dissolve the components in the mixture. After the agitations, it was left resting until all the bubbles of the solution disappeared. Finally, the solution was ready and the electrodes were prepared.

Conventional electrodes: One drop was deposited over the graphite electrode (Figure 5.3). When the membrane was dry, another drop was deposited. This procedure was repeated every 5 minutes until the membrane had a sufficient volume of it, after an hour of droplets depositions.



Figure 5.3 Electrode mixture deposition in conventional electrodes.

The deposition has to be very carefully done, in order to avoid the formation of bubbles. Any bubble deposited would have remained in the polymeric membrane and would have caused instability in the sensors response.

Tubular electrodes: The general mechanism was similar, making additions drop by drop and waiting until the polymer membrane was dry. The main difference is that, as they are tubular, the zone that is used for determining potentials is the channel in the middle (see Figure 5.4), where the solutions flow through. The surplus solution that emerged from the other channel was cleaned out in order to remove it from the non-sensitive part of the electrode. Therefore, once every drop was deposited, it had to be slightly and constantly blown to make the solution go through the channel and that it impregnates the walls of the channel. The amount of electrode mixture solution added was equal for all the electrodes.



Figure 5.4 Tubular electrodes.

Once the four electrodes had a consistent layer of polymeric membrane, they were left 24 hours at room temperature for drying.

5.4.2. Conditioning

After the electrodes were finished, they required conditioning. This means that the polymeric membrane with the ionophore has to be exposed to the cesium ions for certain time in order to improve the selectivity towards this ion. The importance of this step is that if the electrodes are not properly conditioned with the solutions they have to recognise, their capacity for detecting such metal ions gets significantly lowered. To achieve that, electrodes were exposed to cesium 10^{-2} M standard solutions as it was detailed in previous works [14], [15].

In the present work, cesium standard solutions were prepared from cesium nitrate (CsNO_3) for all the tests and for the electrodes conditioning. The reagent used for making the carrier or ISA solution was tris(hydroxymethyl)amino-methane (TRIS). A buffer solution at pH 7,4 prepared with TRIS and HCl, with a concentration of 10^{-1} M, was used as the carrier or ISA for all the cesium electrodes tests

executed. As done with the other heavy metal solutions, 100 ml of each solution were prepared by dilution of the former concentration.

Table 5.6 Cs(NO₃) standard solutions.

Concentration	10 ⁻¹ M	10 ⁻² M	10 ⁻³ M	10 ⁻⁴ M	10 ⁻⁵ M
Volume	100 ml	100 ml	100 ml	100 ml	100 ml

Usually the conditioning of the electrodes is done by exposing them to a 10⁻² M solution continuously for 24 hours [14]. In the conditioning performed for the four electrodes, the exposition of the electrodes to the 10⁻² M standard solution was elapsed during 48 hours to be sure that the electrodes were properly conditioned.

5.5. Cesium electrodes calibration

5.5.1. Cesium ISEs external calibration

External calibration was performed with the conventional electrodes connected to the pH-meter following a similar procedure than previous external calibrations. The electrodes were immersed in 20 ml of ISA solution. Gradual additions of standard solutions were done and potentiometry values were recorded. The calibration was performed with less concentration points due to the excellent previous experiences with other electrodes. The results obtained with the conventional electrodes are shown in the section 64.

The tubular electrodes were connected to the pH-meter for their external calibration. Once the peristaltic pump was connected, the solution flow passed through the electrodes and the acquisition program was started, values were noted down. The results obtained were extremely irregular with oscillations of several mV. Therefore, the tubular electrodes were considered defective and their external calibration was not performed. Nevertheless, they were conserved to check if the variation observed in the pH-meter was also observed when calibrated though the SIA equipment.

5.5.2. Cesium ISEs internal calibration

After the external calibration proved that the electrodes were successfully built and that they were functional, internal calibration was executed. All the electrodes were connected in series in the next order: T1, T2, Reference, C1, C2 (see Figure 5.6). Tubular electrodes were still tested to see if the results obtained in the pH-meter were confirmed in the equipment. Additionally, the channels for data acquisition were activated.

Signal cables that connected the electrodes with the SIA system were checked again and also for the internal channels of the equipment. All four electrodes were connected and all the values were recorded. The maximum of each determination was noted down for calibration, as executed with previous calibrations. Results evaluation is shown in the section 6.6.

Once everything was configured, the internal calibration was executed as usual in previous tests. Solutions were determined in an increasing order of concentrations, from 10^{-5} M to 10^{-2} M. First attempts of internal calibration failed. The oscillations of the signal were too high to evaluate the resulting potential (see Figure 5.5).

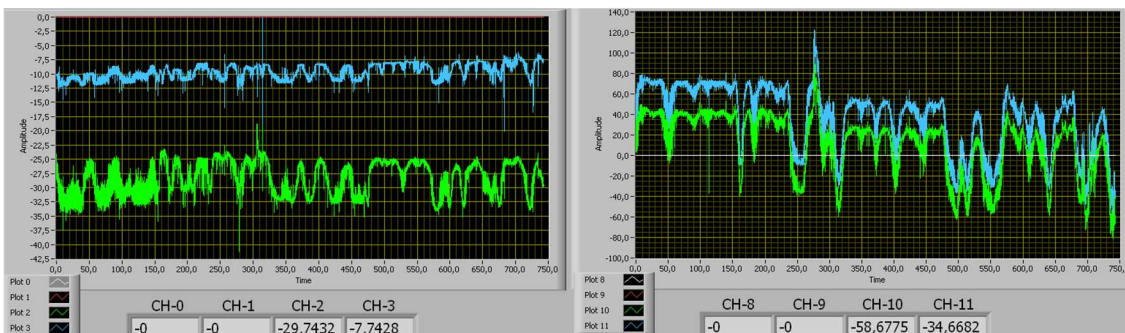


Figure 5.5 Cesium failed internal calibration.

Therefore, a different approach was considered in the next calibration. The main difference between this calibration and the previous one was that in this one, solutions were not being transferred through the system burette and valves. The reason is that the tubular electrodes have to work at constant flow. Finally, they were calibrated with the peristaltic pump directly connected to the electrodes. It is considered as internal calibration because the electrodes were connected to the SIA system. Values were generated internally and recorded with connections.

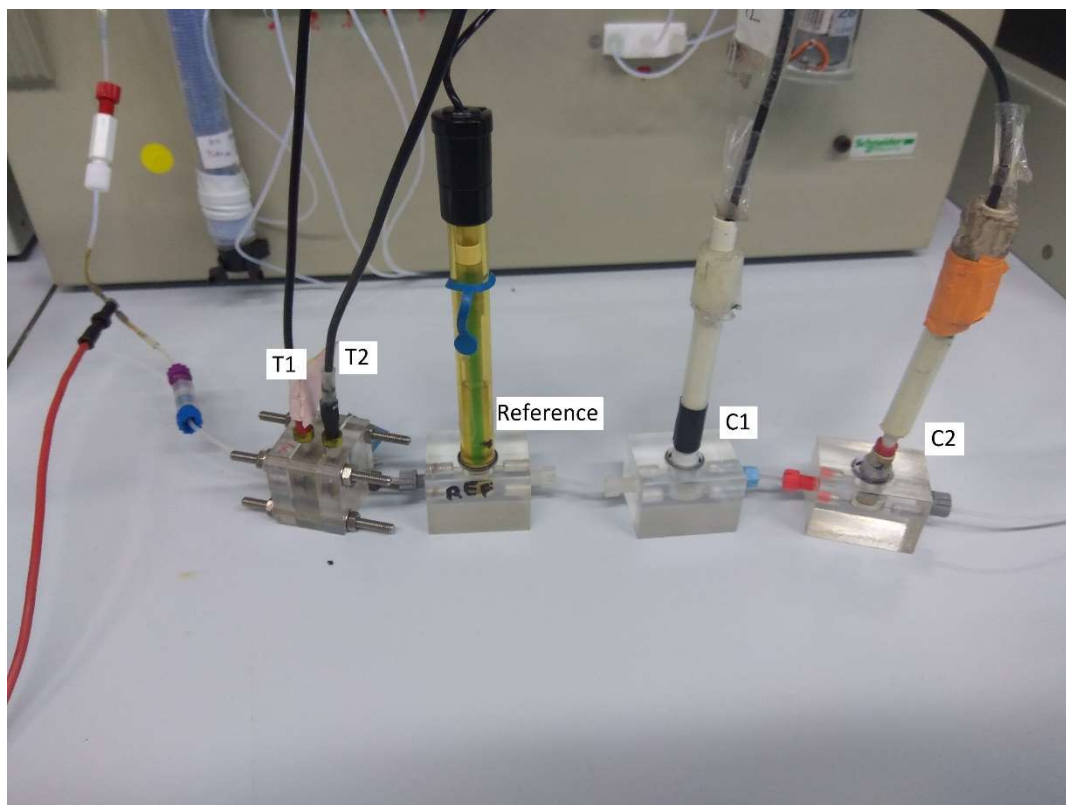


Figure 5.6 Cesium ISEs calibration.

The electrodes connected to the equipment generated much oscillation, especially the tubular electrodes. Nevertheless, average values could be identified among the oscillation and taken as the value determined for each concentration added.

The calibration curves were calculated. Their analysis and evaluation are done in the section 6.6. Considering that some of the electrodes responded proportionally to the solution additions and performed successfully, the biosorption of the cesium was intended with the constructed electrodes.

5.6. Monitoring of the cesium biosorption process

5.6.1. Grape stalk preparation

Many investigations have been made to find new waste materials to be used as sorbents (see Table 5.7). The target material should be a cheap material, an abundant material easy to purchase and with high absorption capacity. In the present work, grape stalk was used as biomass for the cesium biosorption. It was already investigated in previous works and its capacity for absorbing different heavy metals was proved [8].

Table 5.7 Absorption capacity of different biomass [14].

Absorbents	Qmax mg Cs/g absorbent	Ref.
Azolla filiculoides	70,43	[44]
Pine	2.45 (natural pine)	[45]
	2.83 (treated pine)	
Coconut lignocellulose	32	[46]
	65.7 (NiHCF)	
Nut shell	0.52 (NiHCF)	[47]
Basil seeds	160	[48]
Persimon	101,00 (H ₂ SO ₄)	[49]
Brewery waste	10,1	[50]
Funaria hygrometrica fungus	6	[51]
	17 (NaOH)	

The preparation of the grape stalk followed the next steps:

- Agriculture grape stalk waste was grinded until the stalk segments had a size between 0,5 and 0,8 mm.
- Grape stalk was washed with distilled water. This process was made with a magnetic stirrer inside the recipient. Every 30 minutes the water, which dirty with many particles, was replaced. This process was repeated until the cleaning water was transparent and clean after the 30 minutes washing. The total time elapsed for the grape stalk washing was of 8 hours.
- Grape stalk was filtered, recovered and dried at 110°C for 24 hours.

Note: Later, during the realisation of the tests, it was observed that the solutions became a brownish after crossing the absorption column. Because of that, it was considered that the washing stage wasn't long enough. It was observed that, during the washing stages the water turned brownish and cloudy much earlier than the 30 minutes stated. Therefore, faster water removals should be done to drag out the solid particles. For instance, a washing elapsed during 8 hours but changing the distilled water every 20 or 15 minutes.

5.6.2. Column preparation

The column used for the absorption was an Omnifit column with a diameter of 1,0 cm and a height of 10,0 cm. The column was placed vertically with a support. A water stream with slow flow was

introduced from the bottom of the column to the top, which was left uncovered. Then, 1,3 g of grape stalk previously washed and dried were introduced inside the column while the water level was slowly rising inside the column. The grape stalk was introduced inside very carefully trying to not create any air bubbles that can cause a great distortion in the potential determination and create preferential flow paths.

Once the column was full of grape stalk and water, the upper part was covered with the corresponding filter. The upper part of the column, over the filter, was left opened (see Figure 5.7) while performing other preparation tasks in order to keep washing the stalk and also to avoid leaks because of the gravity.



Figure 5.7 Absorption column purge.

5.6.3. Calibration

The biosorption process was performed as in previous works [14], [15]. A calibration of the system was done with cesium solutions of 10^{-5} M, 10^{-4} M, 10^{-3} M and 10^{-2} M solutions. The solutions were sent from the recipients to the system with the peristaltic pump, but without passing through it.

The peristaltic pump was set (Figure 5.8), with three different conduits transferring cesium (A), TRIS buffer (B) and ultrafiltered water (C).

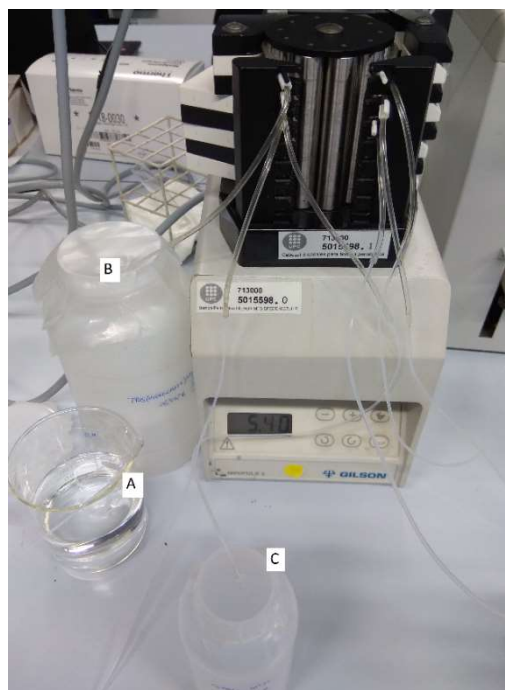


Figure 5.8 Cesium biosorption setup.

A: Ultrapure water

B: TRIS buffer

C: Cesium solution

With the present configuration, the system could be previously calibrated with the carrier and the solution placed in the C input, while the column was still being purged and refilled with distilled water.

As occurred during the first calibration, the oscillation was very high. Nevertheless, the calibration was performed successfully with the four cesium ISEs constructed by taking as reference the average values. All the values were recorded to compare the performance of the different sensors. Calibration curves and evaluation of the results are shown in the section 6.7.

5.6.4. Biosorption process

Once the calibration was performed, the parameters were analysed to confirm that the system was stable and that the biosorption process could be performed. TRIS buffer was connected to the column in order to remove the remaining water before the absorption. The reason is that remaining distilled water could cause oscillations in the electrodes.

Then, the solution input (C in the figure above) was connected to the column. The output of the column and the TRIS solution were joined in a manifold (see Figure 5.9) and sent to the SIA system. With this, the cesium solution flowed through the column and entered the system with the TRIS

solution as a carrier. Both channels were transferred at the same flow rate of 30 ml/h. All these conduits were propelled by the peristaltic pump.

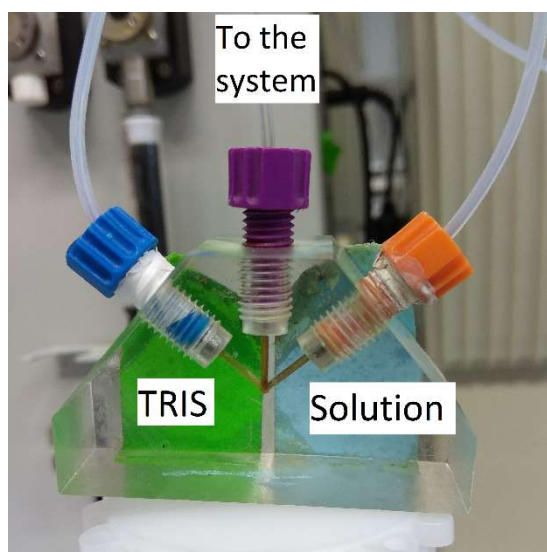


Figure 5.9 System manifold.

Once the connections were done, the absorption process was executed, transferring cesium solution of 70 ppm through the column to its saturation point. The monitoring of the process was successful, recording the variations of the cesium concentrations. The results are analysed in the page 68.

5.6.5. Desorption process

Once the sensors signals reached a high and steady value and the fixed bed column was considered to be saturated, desorption process was studied. In order to do that, the peristaltic pump was turned off. The cesium solution of 70 ppm was disconnected from the column and in its place TRIS solution was connected. In order to make the grape stalk expulse the cesium absorbed for its quantification, TRIS solution transferred through the column was acidified to pH 3 with nitric acid (HNO_3). The biosorbent can release the metals absorbed by lowering the pH to 3 inside the column [52]. The solution is not used with a pH lower than 3 because it might damage the grape stalk. With this, both conduits joined in the manifold were transferring TRIS buffer at pH 7,4 and TRIS buffer at pH 3 though the column.

Cesium was gradually released from the grape stalk and detected by the sensors. The potential values obtained by the different sensors through the process are analysed in the page 70.

5.7. Equipment optimisation

5.7.1. Equipment set up

During the test experiments performance, a series of conclusions were made about how to set the equipment and to execute the test in order to improve the signal quality. In this section, a description of the improvements is made. The observations were as described below:

Bubble trap: When the SIA is working with the burette, the flow generated by its movement is a laminar flow that causes little interferences and reduces the noise. For the experiments tested with the peristaltic pump, it was observed that the forward-backward movement of the pump created certain oscillation in the solution flow. This oscillation was being transferred to the electrodes. In order to minimise this problem, a bubble trap was built with two pipette tips of different size (Figure 5.10).

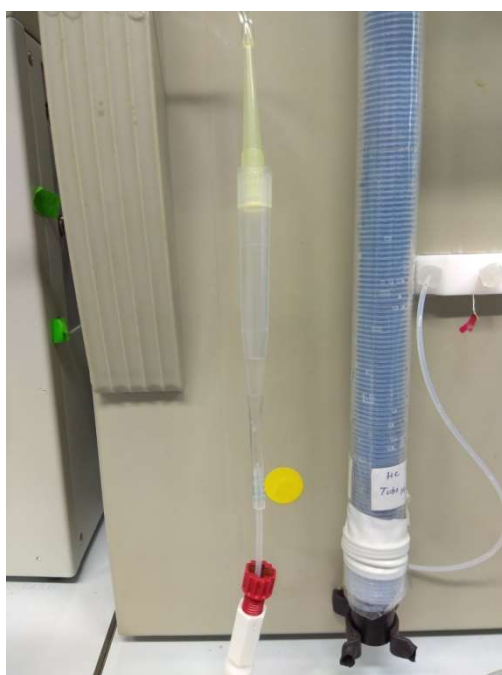


Figure 5.10 Bubble trap.

ISE positioning: The conventional ISEs used are placed inside a PMMA support. The union between the ISE and the support is done in a way that certain space is left in between, in order to let the solutions flow through it (Figure 5.11). This volume has to have a height between 1 mm and 2 mm, big enough to create a dilution zone. If the dilution space is too big, the solution needs excessive time to fill it, pushing the carrier solution and reaching the highest concentration within the dilution space.

On the other side, if the electrode is fully introduced into the gap, the solution flows through the sides of the electrodes and the detection is not successful.

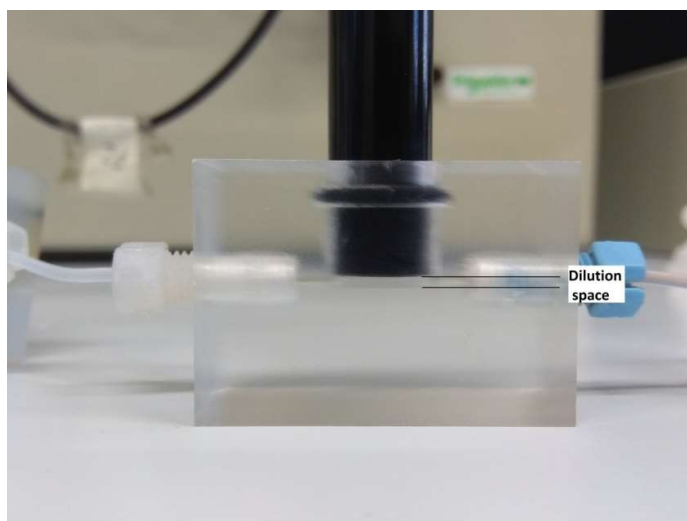


Figure 5.11 ISE dilution space.

Because of the dilution space, the air inlet into the system had to be totally avoided. The presence of bubbles inside the conduits can be accumulated in the ISEs dilution space. These bubbles create a great distortion in the potentiometry lecture and hence, they have to be removed.

In previous works it was determined that the best performance was obtained when the electrodes were positioned with certain inclination respect to the floor [13]. Results were slightly better when placing the electrodes with an inclination of 45° (Figure 5.12).

When used within the SIA equipment, the ISE and the reference electrode were placed in series, with the reference electrode receiving the solutions first and the ISE secondly. Trials were done in order to detect if the order of the electrodes position could affect the potential detection. No significant differences were identified

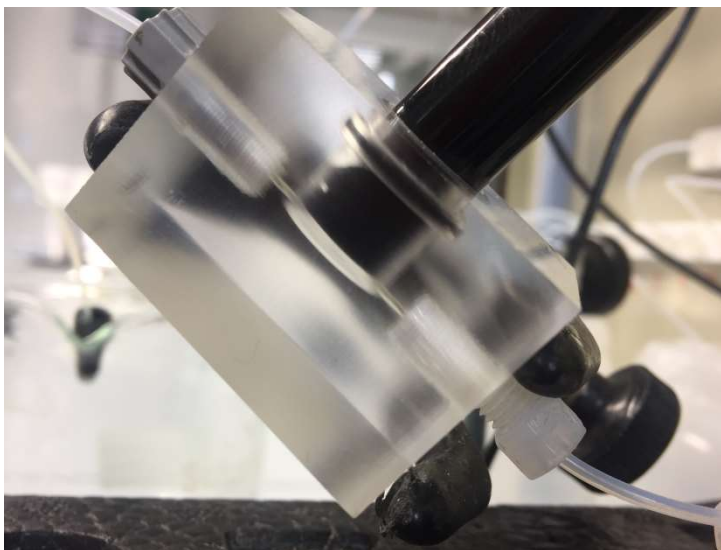


Figure 5.12 45° ISE positioning [42].

5.7.2. Acquisition channels testing

Before the tests were performed, all the wires functioning were checked with a tester. It was confirmed that all them worked properly. Additionally, with a potential simulator, the equipment was induced with a current of 0 mV, 200 mV, 400 mV, -200 mV and -400 mV. An acquisition through the Labview was programmed to record the values obtained by the system during 15 seconds.

The differences between the induced values and the ones detected by the equipment were measured for every acquisition channel (Figure 5.13). All the channels had a slight difference respect to the induced values yet the differences were constant respect the reference value. Because of the stability of the signal, the slight differences between the values induced and the values obtained were considered not significant. It has to be considered that for every test executed, a calibration was performed. Therefore the deviations present in the system were affecting both results in the same way. Therefore, the absolute value obtained in an experiment is not significant. Only from the comparison between the value and the calibration curve conclusions can be made.

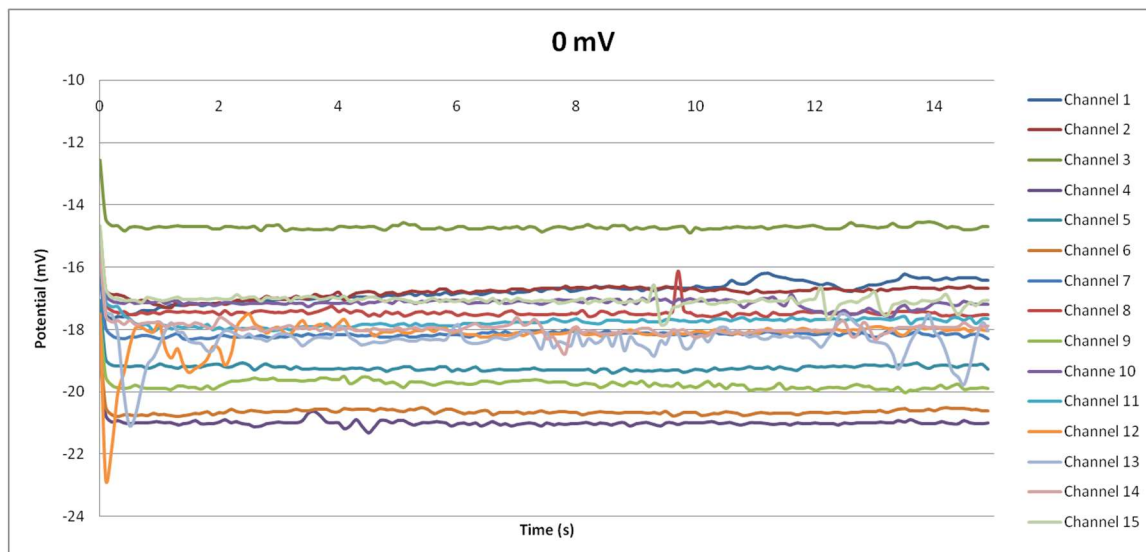


Figure 5.13 Channels deviation checking.

5.7.3. Noise reduction

The oscillation of the signal during the tests was minimal in most of the cases. Values were regular and usually considered as good when the oscillation was less than 0,5 mV in 1 minute. Nevertheless, internal and external calibrations showed a significant difference in signal stability. The potential measure within the SIA equipment caused a bigger noise in the potential detection and, therefore, lower signal quality. Additionally, the oscillations were exponentially increased when testing all the electrodes. In order to solve these inconveniences, different tests were performed along the duration of the project. Some test were simple trials while others required changing more elements, nevertheless all the things that contributed to a reduction of the potential oscillation are described below, test by test.

Insulation in a Faraday cage: Whether the tests are performed externally in the pH-meter or internally in the SIA, the electrodes are placed in the outside of the equipment, without any protection. It was observed that any influence in the environment, such as a person standing next to where the electrodes were placed, caused oscillation on the values of potential. These influences showed that the equipment is highly sensitive to its environment and changes in the surroundings can have significant influences.

In this context, the electrodes were isolated inside a metallic box, acting as a Faradays cage, and a determination was executed. The results obtained increased the fluctuation of the potential and worsened the situation. It is considered that the metallic box acted as an antenna instead of a Faradays cage and the idea was discarded.

Electric net influences: When connecting a laptop to a near plug, the equipment experienced a sudden decrease of the potential in a middle of a determination. Because of this discovery, no more high power consuming equipment were connected in the shared plugs.

Electrodes polished: After several tests with the copper ISE, the results started being worst, fitting less in the calibration curves and generating lower slopes than expected theoretically. With a thin sandpaper the electrode was polished and the results improved to the ones obtained initially. Since then, electrode was polished periodically every 10 determinations.

Solutions caducity: The standard solutions prepared for every heavy metal testing were used only during two weeks. After that period, if there was any remaining solutions, they were discarded as waste to avoid that any possible degradation suffered by the solutions could affect the results.

Solutions similitude: Carrier solutions were made with potassium nitrate flushed with ultrafiltered water. It was proved that pure water is a source of variability compared to ionic solutions. After certain copper tests, metal standard solutions were flushed with KNO_3 instead of ultrafiltered water. Because of that, all the solutions were always prepared together: potassium nitrate with ultrafiltered water and standard solutions with potassium nitrate. With this, the variations of potential between the carrier and the solutions were minimised.

Considering this concept of same ionic solutions, reference electrode was filled with the prepared carrier solution instead the commercial one in order to obtain the maximum similitude between all the solutions.

Reduction of the concentration range tested: Initially, calibration curves were done by determining the potential of standard solutions of concentrations from 10^{-5} to 10^{-1} M. After the initial copper calibrations, it was observed that the wrong results obtained in the calibration were caused in their majority by the concentration 10^{-1} M. Therefore, it was considered that the concentration was too high and almost out of the linearity range. From that point all the calibrations were made without this concentration which generated one less point in the curves.

5.7.4. Complexes formation control

After some problems in copper calibrations, it was considered that the solutions may be forming complexes and thus lowering the amount of free ions present in the solution, with this affecting the potential determination. To prove or reject this hypothesis, the pH of the standard solutions was checked. Once the pH was found to be around 4, the complexes formation at the measured pH was researched with the free software for chemical equilibriums Medusa.

The equilibrium charts obtained for the different concentrations of copper solutions is shown in the next figures.

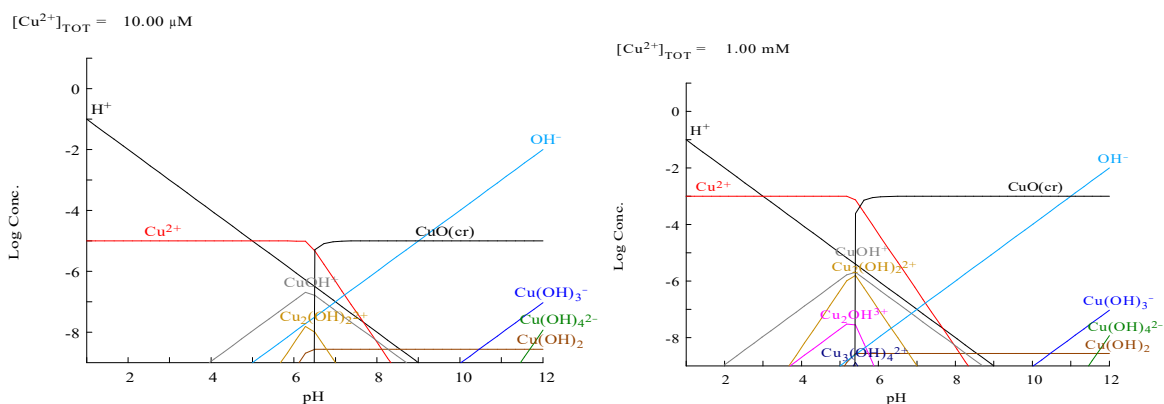


Figure 5.14 $[\text{Cu}^{2+}] = 10^{-5} \text{ M}$ and $[\text{Cu}^{2+}] = 10^{-3} \text{ M}$ equilibrium chart.

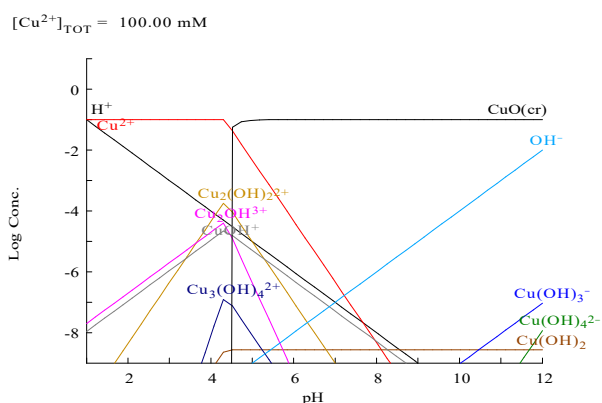


Figure 5.15 $[\text{Cu}^{2+}] = 10^{-1} \text{ M}$ equilibrium chart.

Considering the graphics obtained, it was considered that some complexes may be being formed in the most concentrated solution, because the solution pH was 4 and the complexes formation occurs at pH 4,5. Therefore, an acidification was performed to pH = 3 for all the solutions and then a calibration was attempted to check if the potential detection improved. It resulted in higher inaccuracy with a much worst potential values, so the formation of complexes was discarded.

5.7.5. Repeatability

Repeatability tests were executed with both copper and cadmium ISEs separately. Copper nitrate solution of 10^{-5} M was tested 10 times consecutively. Between the determinations, 2 cleaning steps were performed. The cleaning steps consisted in filling the burette maximum capacity (5 ml) with carrier solution and introducing the dissolution through the system to remove the remaining sample.

The performance of this test showed that the same sample caused different potential values. Only after the fourth determination, the values obtained started being stable.

This was correlated with what was found in the literature [11]. Trials with colorimetry tests proved that there were needed 20 ml to pass through in order to totally clean the system. In our tests, every determination spent 5 ml of solution (3,75 ml standard solution + 1,25 carrier solution). That is the reason of why the repeatability was correct only after the fourth repetitions. Traces of previous samples tested were still in the system and the electrodes were not used to the solution. Once equilibrium was reached, repeatability obtained was very high.

Considering the volume needed for total cleaning, future tests were adapted. Calibrations and all the trials performed after this test were composed by 4 cleaning stages between samples determination. This reduced the hysteresis of the system.

After the repeatability tests, a calibration was performed which included repeatability evaluation. This means that in a single calibration, each solution was analysed 5 times before determining the next one (see section 6.2.1 clarification). With this, 5 calibration curves were done with the values obtained.

The first calibration was calculated by linear regression of all the first values, the first sample of each concentration. The second calibration was calculated by taking the second sample value for each concentration, and so on until the 5 calibration curves were obtained (see results analysis in the section 6.2.1).

Finally, same calibration was performed with the cadmium ISE, following the same procedure.

5.7.6. SIA software correction

During the dilutions repeatability testing (section 5.3.3) an error in the SIA software was detected. This error caused that during the execution of experiments composed of various acquisition scripts, only some acquisitions were executed. Tests were still performed and the valves and the rest of the equipment performed as usual, but without recording the potential measurements.

Once the acquisition bug was detected, it was fixed and consecutive acquisitions could be performed. With this, long experiments with several scrips could be executed. For instance as a calibration, ten dilutions and another calibration all consecutively, were designed to perform the test described in section 5.2.3.

5.8. Online connection

Before facing the SIA system connection, different programs were considered for the data acquisition before starting with any of the experiments. The goal was to determine which of the software from different equipment available in the laboratory was more suitable for online connection and data sending.

The SIA system with the Labview software were tested (see section from page 19). Additionally, two external pH-meters were used for data acquisition in order to see if the data generated was easier to modify, treat and send through the net to the RAdb.

Orion 5 Star multifunction-meter was tested. The data acquisition was executed and a calibration was performed successfully. The data generated was investigated in terms of accessibility for data processing and data transfer. The files generated by its software, Star Navigator, were stored in different files within a database. The data was difficult to access and the version of the software installed was too old. Additionally, other limitations of the multifunction-meter were that only one sensor could be connected at the same time. Therefore, this option was discarded.

pH-meter Crison GLP22 was also tested. This equipment was used for the external calibrations performed in this test and worked with good accuracy. The inconvenient of this equipment has an older version of the software via RS232 which makes difficult to connect. Data had to be noted down manually and for this reason it was discarded.

Subsequently, from the collaboration with the Norwegian Institute of Water Research (NIVA), the conditions of the communication with the RAdb were established in order to synchronize both technologies.

5.8.1. Frequency

The volume of data generated by the SIA system is very high. The configuration of the data acquisition used for the realisation of this project is to generate an array of values every 0,1 seconds. This means that for each of the 16 channels available in the equipment, the data acquisition will create 36.000 values every hour. This amount of data is only useful when analysing fast events, usually in the laboratory. The future use of this technology, when fully developed, would be to monitor some water environment, like the sea coast or the river basins.

Additionally, the aim of the NIVA RAdb is to control the level of contaminants along the time in a fixed position and to collect environmental information to detect risks stressors.

For the reasons stated, a low frequency such as every 5 or 10 minutes is sufficient. Therefore, for the connection of the equipment with the database, the frequency must be changed. In order to achieve this, different options have been considered.

First, the increase of the period of data intake by the Labview software (see page 20) was tested. Instead of generating data points every 0,1 seconds, potential could be recorded by the system only once every 1, 5 or even 10 minutes. 1 minute was tested and the data value was successfully recorded once in a minute. The inconvenient of this solution is that the value recorded would be very punctual and may not be very representative of the solution situation. To avoid this problem, the averaged values used to generate that data should be changed to be very high. In example, instead of averaging 500 values every 0,5 seconds, the average could be calculated over more values. On the other side, this calculation could use much of the computation capacity of the system when recording the value.

The second option considered was to create a script to read data values every specified time and send them to the database. It could be done directly from the operative system (OS) or from the same Labview software. The latter one was considered to be the best solution, because it offered an integrated solution within the system. The program could be modified and the option of data sending added.

5.8.2. Data format

The .txt file generated by the software is composed by data lines, where each sensor stores the data in one column (Figure 4.4). The resulting document is filled with the values in columns, even for the sensors that are not active during the execution of the test. The inactive sensors fields are filled with a -0,0000 mV value.

For the automatic RAdb processing of the values, the system could not process the inactive sensor values, because they could cause a miss lecture of the potentials and so, an incorrect determination of the potential risks. For this reason, the elimination of these data columns was specified.

Additionally, the database needed the date and time to relate the data processed with the time they were generated. Because of that, another column was considered to be added with the time and date of each data line in the next format: hh:mm:ss dd/mm/yyyy. With this, the data could be correlated with time and, therefore, establish a study of the evolution of the pollutants concentration of the location site of the sensor.

All the improvements in the data files format were recorded. Time format was added in seconds as part of the program improvements. The rest of the modifications implied deeper modifications and could not be performed during this project.

5.8.3. SFTP: Secure File Transfer Protocol

For the data transmission, a Secure File Transfer Protocol (SFTP) was established and tested. The connection of an SFTP is relatively simple and the codification of the files makes it a secure way to perform the data transfer.

The NIVA procured a dedicated server for the transmissions made along the duration of this project. From the EEBE (Barcelona), the Filezilla software was selected as a SFTP program. It was installed in a desk laptop and in the SIA control computer for different testing. The SFTP was successfully performed with different handwritten .txt files from the desk laptop. These files were used for the data transmission testing but also for format testing, in order to see if the RAdb could process the information sent (Figure 5.16). The files could be successfully transferred and processed by the RAdb.

```
Date/Time,Zn,Fe,Cu,All Units in ppb  
01.02.2018 01:19:11, 200, 200, 200
```

Figure 5.16 Test file for SFTP.

Later, the same test was attempted from the SIA control computer. Filezilla had to be installed in an older version because the OS of the computer was too old. The transfer program could not be updated enough for performing an SFTP. Because of that, a new computer was acquired at the end of the project and the Labview software was updated, along with the Filezilla.

6. Results analysis

6.1. Cupper external calibration

The stability results obtained in the external calibration with the pH-meter was good and for the potassium nitrate solution the variation was less than 0,2 mV/min. The same results were obtained after each addition.

Table 6.1 Cupper external calibration results.

Concentration added (M)	Volume added (μ l)	Total Volume (ml)	Concentration (M)	log C	E (mV)
0	0	20	0	-7	90
0,001	25	20,025	1,25E-06	-5,9036	109,2
0,001	50	20,075	3,74E-06	-5,4276	123
0,001	100	20,175	8,67E-06	-5,0618	134,2
0,001	250	20,425	2,08E-05	-4,6818	145,9
0,001	500	20,925	4,42E-05	-4,3545	155,7
0,01	100	21,025	9,16E-05	-4,0383	165,5
0,01	250	21,275	2,08E-04	-3,6820	176,1
0,01	500	21,775	4,33E-04	-3,3637	185,3
0,1	100	21,875	8,88E-04	-3,0516	195,1
0,1	250	22,125	2,01E-03	-2,6973	205,4
0,1	500	22,625	4,17E-03	-2,3795	214,4

The calibration curve was calculated by lineal regression of $\text{Log}_{10} C$ against potential (mV). The results are show in the (Figure 6.1).

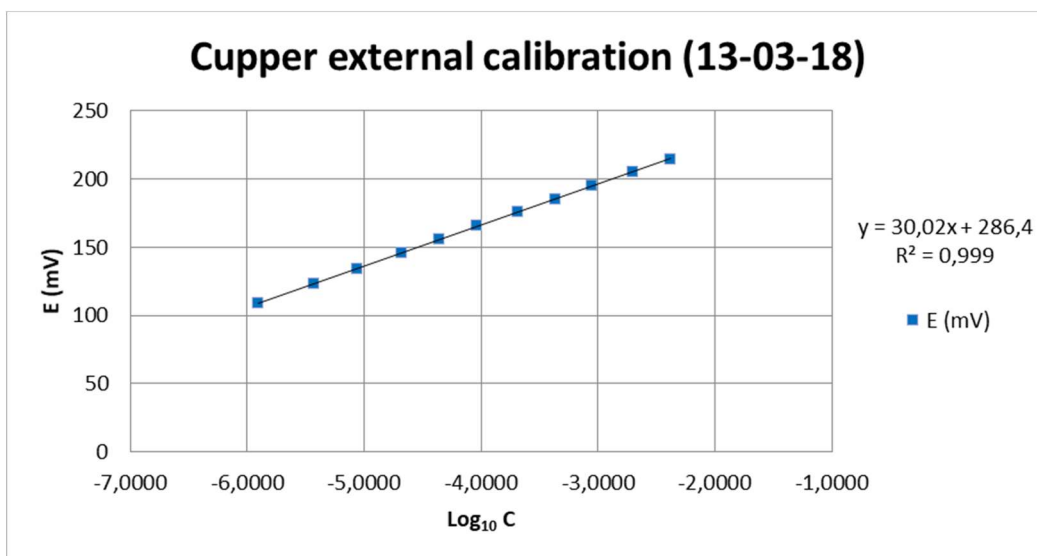


Figure 6.1 Cupper external calibration.

The linearity obtained was very good and fulfils the acceptance criteria. To evaluate the slope, a comparison with the theoretical one was needed. The theoretical result of the calibration can be obtained from Eq. 3.6. With it, the theoretical slope to be obtained is equal to 29,58.

The slope obtained is to be compared with the theoretical to obtain the Margin of Error (MEO) in percentage.

$$MEO = \frac{\text{Experimental slope}}{\text{Theoretical slope}} \times 100 \quad \text{Eq. 6.1}$$

The slope obtained in this calibration was highly accurate and the MEO acceptance criteria is fulfilled.

Table 6.2 Copper external calibration performance.

Acceptance criteria	Requirement	Performance	Results
Linearity	$0.990 < X$	0,999	✓
MEO	10 %	1,5 %	✓
Stability	$X < 0,5 \text{ mV / min}$	0,3 mV / min	✓

As can be observed, the external calibration fulfilled all the requirements. This indicates that the copper ISE was in good conditions and that its selectivity towards copper (II) ions is very high. The behaviour of the electrodes followed the expected Nernstian response.

6.2. Copper internal calibration

With the data obtained with the SIA calibration, the performance of the test was evaluated. The linear regression was calculated (Figure 6.3) from the results as explained in the previous section (Table 6.4).

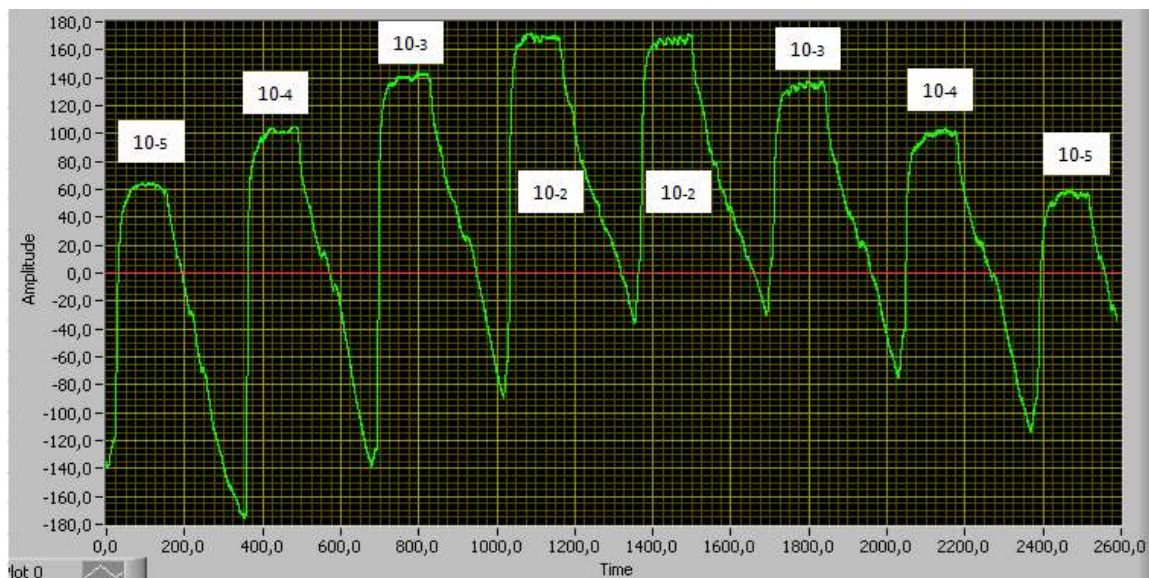


Figure 6.2 Copper internal calibration.

The potentiometry peaks, maximum values acquired during each solution detection are shown in Table 6.3. These values were used to calculate the calibration curve (section 0). Two calibration curves were calculated, from the increasing and the decreasing concentration calibration respectively.

Table 6.3 Copper internal calibration.

Concentration (M)	Log C	E (mV)
Carrier	-	-5
10^{-5}	-5	9
10^{-4}	-4	44
10^{-3}	-3	77
10^{-2}	-2	97
10^{-2}	-2	97
10^{-3}	-3	68
10^{-4}	-4	39
10^{-5}	-5	8

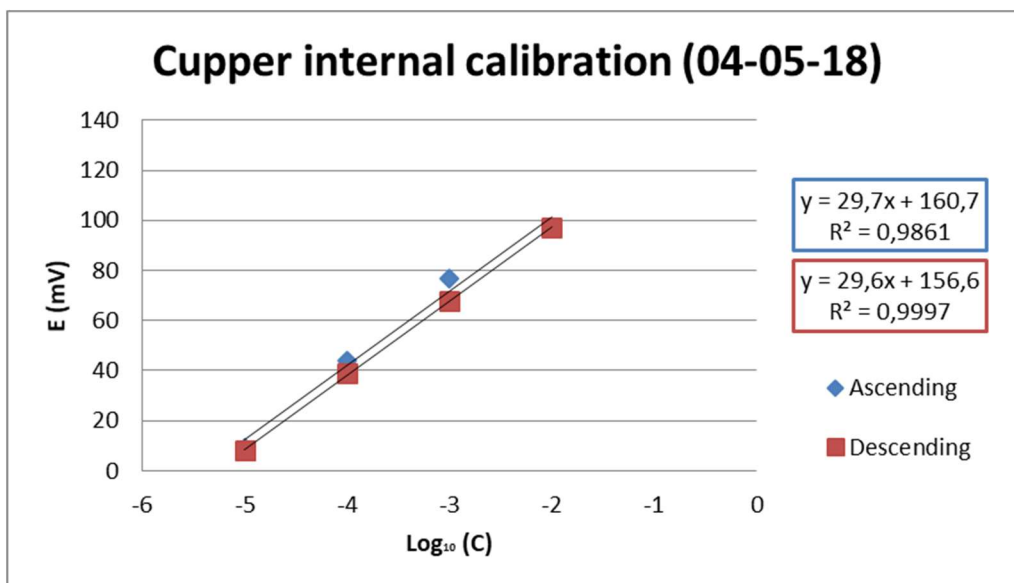


Figure 6.3 Copper internal calibration.

Generally the calibration was performed successfully. No hysteresis was detected, being both curves very similar. The selectivity of the ISE for the copper ions was proved and the capacity of the SIA system to perform an internal calibration for ISE trainings is demonstrated. The method used to achieve these results was improved through different experiments (see section 5.7).

Table 6.4 Copper internal calibration performance.

Acceptance criteria	Requirement	Performance Increasing	Results	Performance Decreasing	Results
Linearity	$0.990 < X$	0.986	✓	0.999	✗
MEO	10 %	0,4 %	✓	0,1 %	✓
Stability	$X < 0,5 \text{ mV} / \text{min}$	0,8 mV	✗	1,1 mV	✗

Linearity was not fulfilled by the first calibration (increasing calibration). Nevertheless, the values are very close to the acceptance criteria and can still be considered a reasonable result. Additionally, the second calibration performed consecutively (decreasing calibration) generated excellent results.

The stability requirement was not achieved by any of the calibration curves. The fluctuation of the values obtained in the SIA system was higher than the fluctuation of the external system. This could be caused by different factors. First, it is possible that the equipment had slight parasitic currents. It has to be considered that such a complex equipment will have higher difficulty to be isolated and, therefore, will generate more noise in the signal. In fact, it was founded that all the internal

calibrations had higher variation than the limit specified despite the good values obtained. It could indicate that the acceptance criteria established was too low for the equipment tested.

Despite the oscillation, the averaged values were very constant and corresponded with the concentration of the solutions, giving a high linearity and low MEO.

The external calibrations were taken as the reference values during the experiments. The pH-meter and the electrodes were free of the possible interferences caused by the SIA equipment. External and internal calibrations were compared to identify possible sources of irregularities that caused differences between the expected potential detection and the one measured in the SIA.

6.2.1. Copper repeatability calibration

The calibration performed with 5 determinations per each concentration was successfully performed (page 54). The values obtained were used to calculate 5 different calibration curves, as explained in the section 5.7.5.

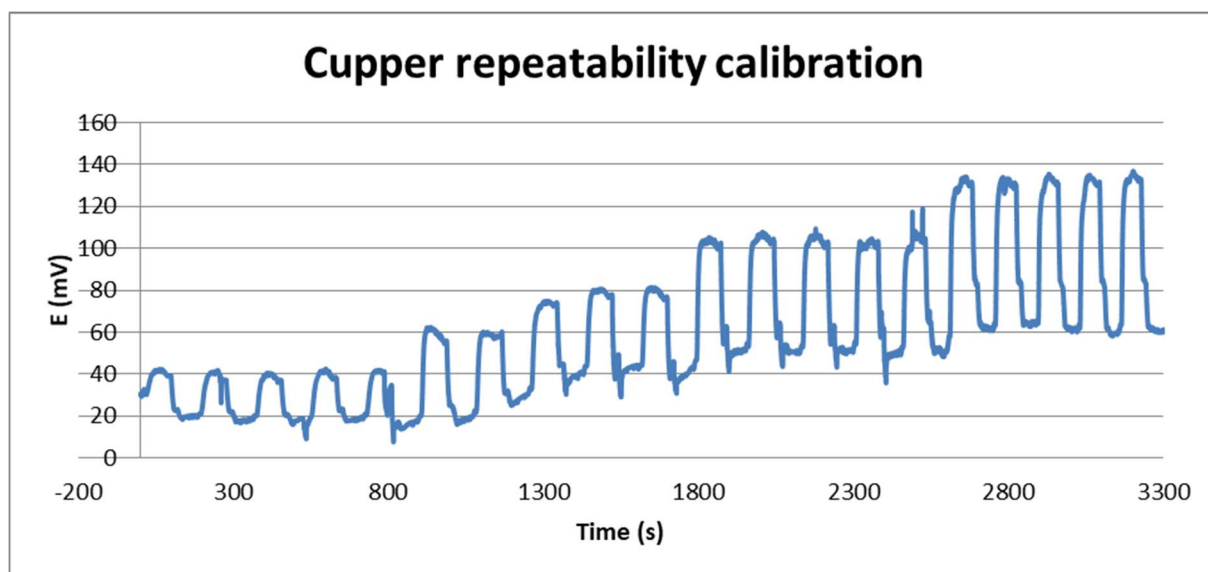


Figure 6.4 Copper repeatability calibration.

Results are presented in the next table. Then, results obtained were evaluated with the defined acceptance criteria.

The Table 6.5 Cupper repeatability calibration.

Sample number	Calibration equation	MOE	Linearity	Linearity acceptance
1	$y = 31,2X + 194,2$	5,4 %	$R^2 = 0,984$	✗
2	$y = 31,6X + 196,1$	6,8 %	$R^2 = 0,976$	✗
3	$y = 31,3X + 197,8$	5,8 %	$R^2 = 0,999$	✓
4	$y = 29,9X + 194,4$	1,0 %	$R^2 = 0,991$	✓
5	$y = 30,7X + 198,7$	3,7 %	$R^2 = 0,992$	✓

The linearity acceptance criteria is not achieved by the first two curves. The margin of error acceptance criteria is fulfilled by all the curves. Nevertheless, the last three curves have significant MOE better values.

Considering these results, the trend observed in the repeatability tests is confirmed by the repeatability calibration. The explanation for this phenomenon is that when analysing for the first time a solution, traces of previous samples are still detected by the electrodes. Once a solution is passed four times with its respective cleaning stages, there are no traces of previous solutions left. Therefore, the values remain constant for the subsequent determinations. This fact was taken into account in the next Cu calibrations.

6.2.2. Cupper dilutions repeatability

In order to ensure that the SIA system did not drifted during the long experiment, a repeatability test was executed with a previous and a latter calibration. With that, the possible drift of the system could be identified and not wrongly attributed to the dilutions. The calibration curves obtained before and after the test are represented in the next equations.

$$Y = 35,7 \times X + 243.2 \quad R^2 = 0,9959 \quad \text{Eq. 6.2}$$

$$Y = 36,7 \times X + 242.9 \quad R^2 = 0,9946 \quad \text{Eq. 6.3}$$

The values obtained in the consecutive dilutions are shown in Table 6.6.

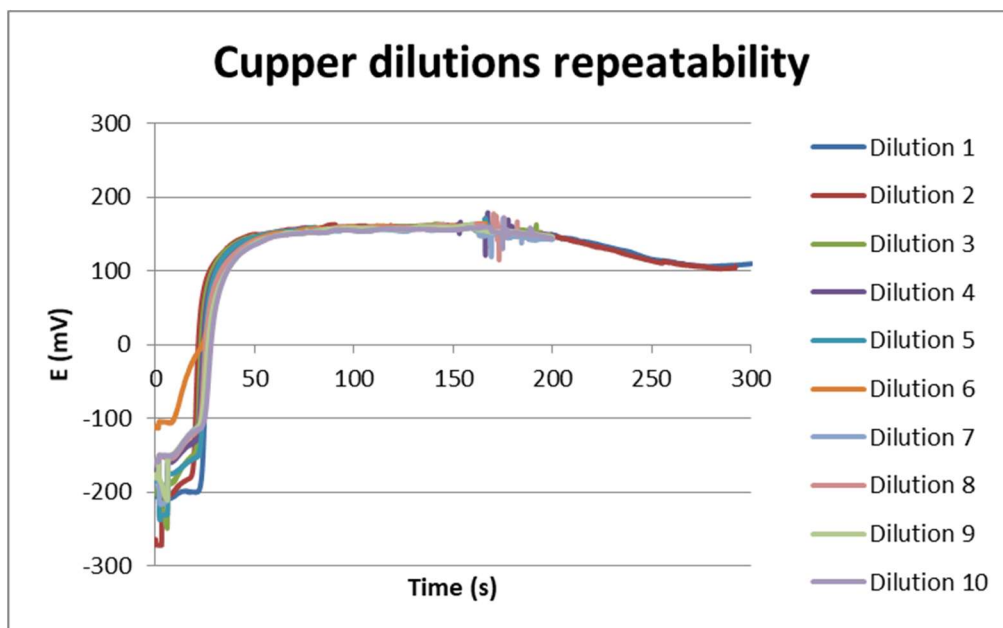


Figure 6.5 Copper dilutions repeatability.

As can be seen, the repeatability of the dilutions was high. All the curves reached the same values and are very similar between them.

The potentials obtained are converted to concentration with the calibration equations (Eq. 6.2 and Eq. 6.3). The concentrations obtained for each repetition are shown in the Table 6.6, in \log_{10} (C) format. In this table, the concentration logarithm obtained is compared to the theoretical concentration of the dilutions made, also in \log_{10} (C) format. Finally, Margin of Error (MOE) is calculated comparing these values.

Table 6.6 Copper consecutive dilutions concentration.

Theo. conc. value	Experimental concentration values (expressed as \log_{10} C)										Cal. curve
	1	2	3	4	5	6	7	8	9	10	
-2,60	-2,33	-2,33	-2,39	-2,39	-2,41	-2,36	-2,47	-2,39	-2,36	-2,44	Initial
	-2,26	-2,26	-2,31	-2,31	-2,34	-2,29	-2,39	-2,31	-2,29	-2,37	Final
MOE (%)	-10	-10	-8	-8	-7	-9	-5	-8	-9	-6	Initial
	-13	-13	-11	-11	-10	-12	-8	-11	-12	-9	Final

As can be seen, the differences between theoretical and experimental values are slight, being less than 10 % for the first calibration curve used and around 11 % with the second one. Therefore, the equipment capacity for preparing dilutions is considered as good.

6.3. Cadmium external calibration

Cadmium external calibration was performed successfully. The values obtained are shown in the next table.

Table 6.7 Cadmium external calibration.

Concentration added (M)	Volume added (μ l)	Total Volume (ml)	Concentration (M)	log C	E (mV)
0	0	20	0	-7	-249,5
0,001	25	20,025	1,25E-06	-5,9036	-235,6
0,001	50	20,075	3,74E-06	-5,4276	-224,2
0,001	100	20,175	8,67E-06	-5,0618	-214,8
0,001	250	20,425	2,08E-05	-4,6818	-204,6
0,001	500	20,925	4,42E-05	-4,3545	-195,0
0,01	100	21,025	9,16E-05	-4,0383	-186,0
0,01	250	21,275	2,08E-04	-3,6820	-175,7
0,01	500	21,775	4,33E-04	-3,3637	-166,1
0,1	100	21,875	8,88E-04	-3,0516	-157,4
0,1	250	22,125	2,01E-03	-2,6973	-147,7
0,1	500	22,625	4,17E-03	-2,3795	-139,2

The values obtained are analysed as explained in the section 6.1. The slope comparisons and the MEO calculations are the same than for the copper because cadmium has same values for z_i . Results are shown in the next figure.

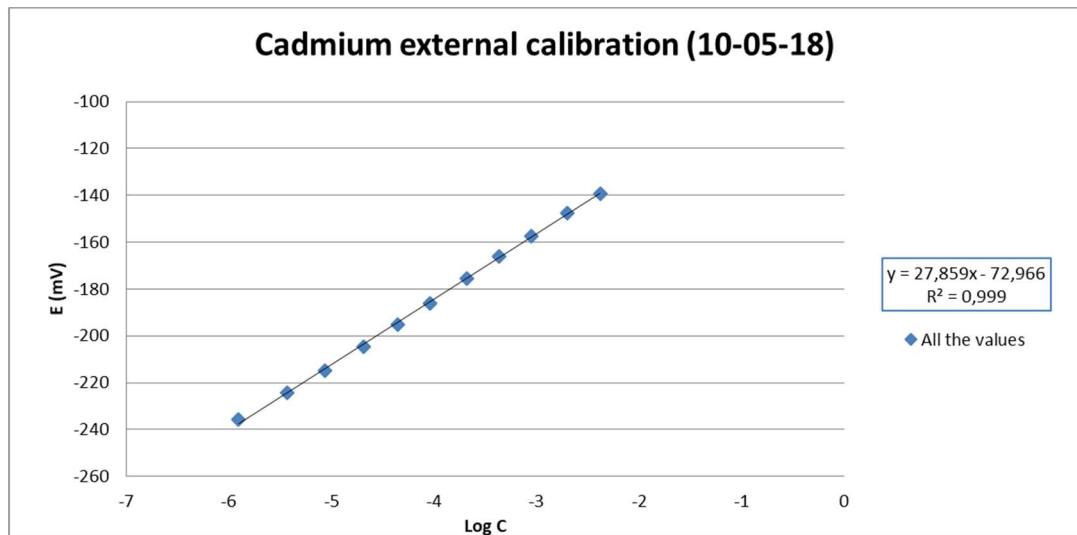


Figure 6.6 Cadmium external calibration.

The parameters of the calibration curve obtained are evaluated in the next table.

Table 6.8 Cadmium external calibration performance.

Acceptance criteria	Requirement	Performance	Results
Linearity	$0.990 < X$	0,999	✓
MEO	10 %	5,8 %	✓
Stability	$X < 0,5 \text{ mV / min}$	0,2 mV / min	✓

As can be observed in the Table 6.8, the cadmium calibration performance was excellent and all the parameters fulfil the acceptance criteria. This indicated that the cadmium ISE determined cadmium ions correctly, following a Nernstian response.

6.4. Cadmium internal calibration

The calibration was executed successfully. The concentrations were determined in an increasing order and, latterly, in a decreasing order.

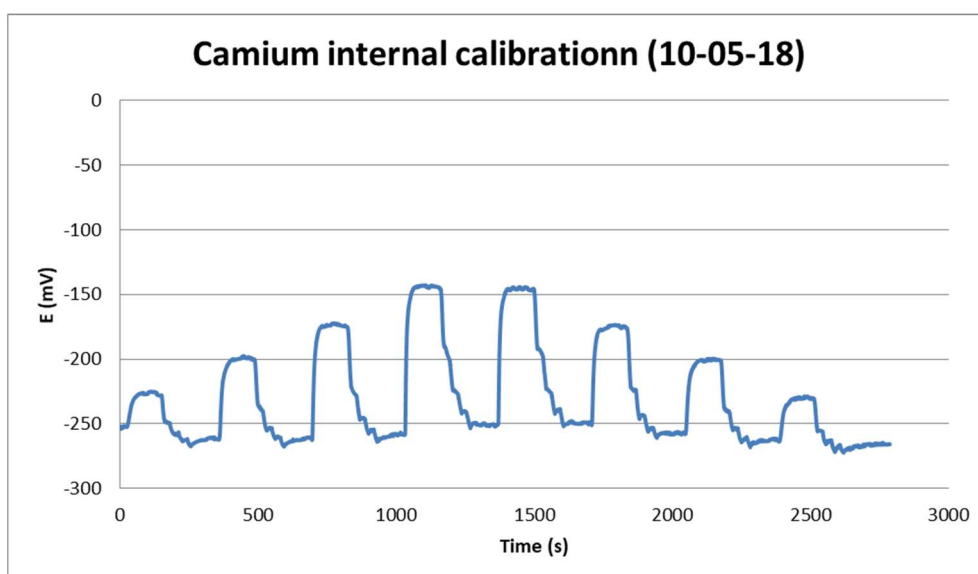


Figure 6.7 Cadmium internal calibration.

The calibration curve was obtained with the maximum potential value obtained with the Cd-ISE (Figure 6.7, Table 6.9).

Table 6.9 Cadmium internal calibration.

Concentration (M)	Log C	E (mV)
Carrier	-	-252
10^{-5}	-5	-225
10^{-4}	-4	-198
10^{-3}	-3	-173
10^{-2}	-2	-143
10^{-2}	-2	-144
10^{-3}	-3	-174
10^{-4}	-4	-200
10^{-5}	-5	-229

With the potential values, the calibration curve was successfully calculated (Figure 6.8).

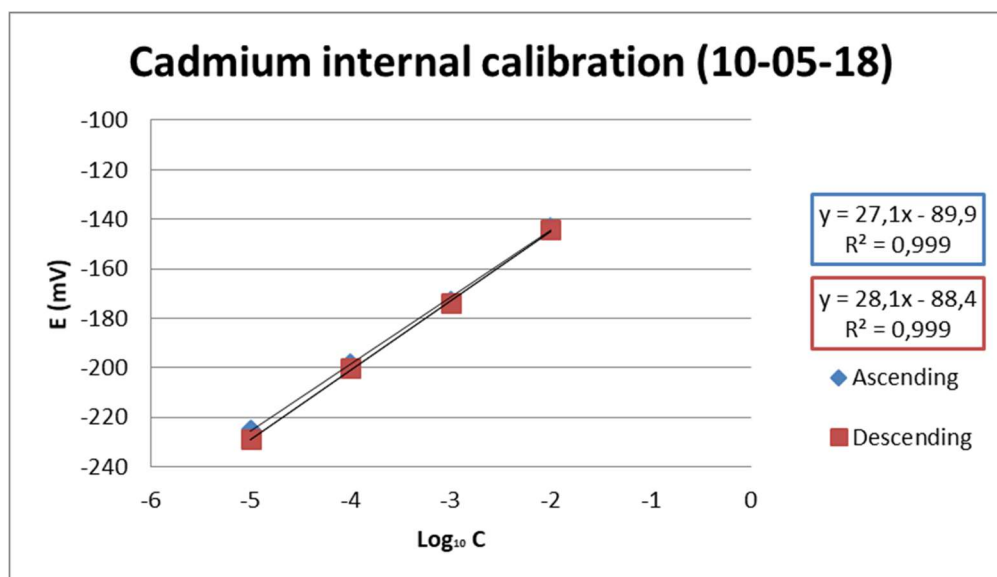


Figure 6.8 Cadmium internal calibration.

No significant hysteresis was detected between the increasing calibration and the decreasing calibration. The determination of cadmium ions concentration by the ISE was very good and the calibration could be performed successfully within the SIA equipment.

Table 6.10 Cadmium internal calibration performance.

Acceptance criteria	Requirement	Performance Increasing	Performance Decreasing	Results
Linearity	$0.990 < X$	0.999	0.999	✓
MEO	10 %	8,4 %	5,0 %	✓
Stability	$X < 0,5 \text{ mV / min}$	0,8 mV	1,1 mV	✗

The linearity obtained with the cadmium electrode was excellent in both calibrations and the values fit the curve perfectly. MEO values of less than the specified requirement indicate that the slope is similar to the theoretical one, calculated in the previous section. However, the stability did not meet the acceptance criteria. This parameter is not accepted neither for the copper or the cadmium in the internal calibrations. As stated in the previous section, the stability of the potential inside the SIA equipment was acceptable and no drifts were identified. The oscillation of the potential was always around 1 mV /min, being even better in some occasions. Because of that, it is considered that the acceptance criteria was established too low for internal calibrations, due to the higher signal noise occurring in these kind of equipment.

6.4.1. Cadmium repeatability calibration

The calibration performed with 5 determinations per each concentration was successfully performed (page 45). The results obtained were very similar to the copper repeatability calibration, showing that repeated determinations of one solution improved the accuracy of the measure.

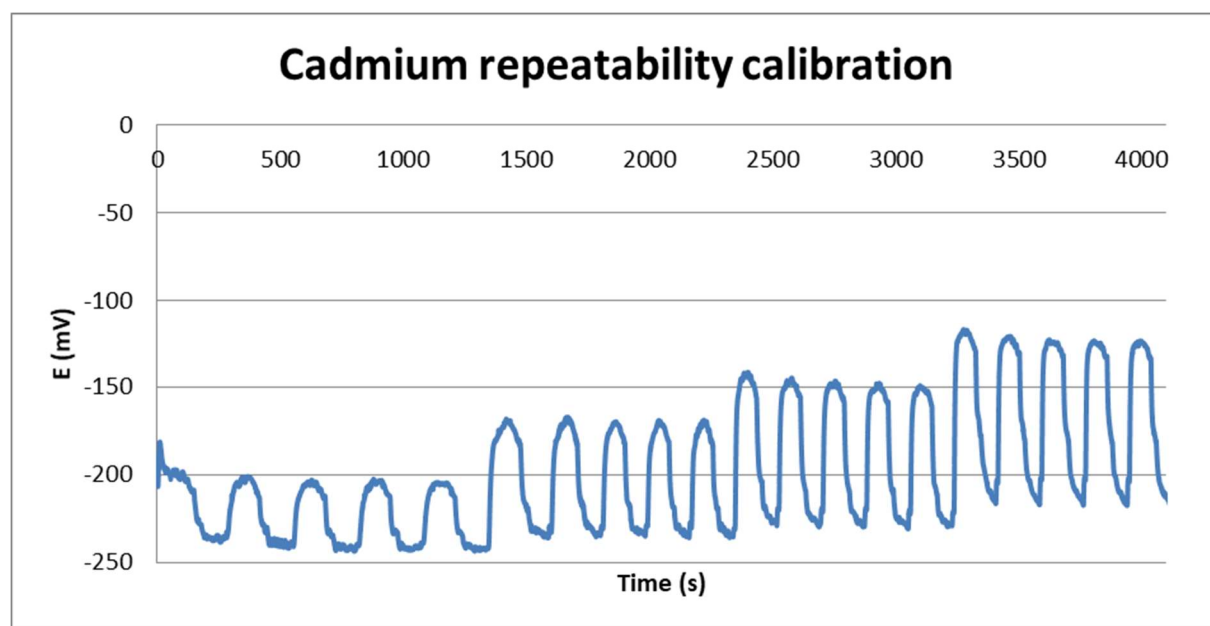


Figure 6.9 Cadmium repeatability calibration.

The results obtained were evaluated with the defined acceptance criteria. Results are presented in the next Table 6.11.

Table 6.11 Cadmium repeatability calibration.

Sample number	Calibration equation	MOE	Linearity	Linearity acceptance
1	$y = 27,2X - 63,8$	8,1 %	$R^2 = 0,999$	✓
2	$y = 27,1X - 65,4$	8,4 %	$R^2 = 0,991$	✓
3	$y = 27,8X - 63,7$	6,0 %	$R^2 = 0,994$	✓
4	$y = 27,0X - 67,0$	8,7 %	$R^2 = 0,994$	✓
5	$y = 27,6X - 64,9$	6,7 %	$R^2 = 0,996$	✓

The linearity acceptance criteria and the MOE is achieved by all the calibration curves. The margin of error obtained is acceptable and similar for all the curves, being the 3rd and 5th the best ones respectively. The linearity is high with $R^2 > 0.99$ and the most accurate value is the one obtained with the 1st curve.

Considering these results, the trend observed in the repeatability tests is not observed here. All the calibration curves showed good parameters and no improvement was obtained after repeating values. In case that the later values would have been different than the first ones, the calibration curves would have been more different from each other.

The favourable point of these results is that despite there is no improvement, there is no decay of the values either. The system proves itself stable and repeated determinations do not affect significantly the next values.

6.4.2. Cadmium dilutions repeatability

Repeatability tests took a considerable amount of time (approximately 3 hours). To avoid any possible drift suffered by the SIA equipment during the execution of the tests, two calibrations were performed, one before the dilutions and another one after. The calibration curves obtained are represented in the next equations.

$$Y = 27,4 \times X - 79,6 \quad R^2 = 0,9981 \quad \text{Eq. 6.4}$$

$$Y = 27,3 \times X - 80,2 \quad R^2 = 0,9978 \quad \text{Eq. 6.5}$$

The dilutions were performed correctly, as can be seen in the figure Figure 6.10.

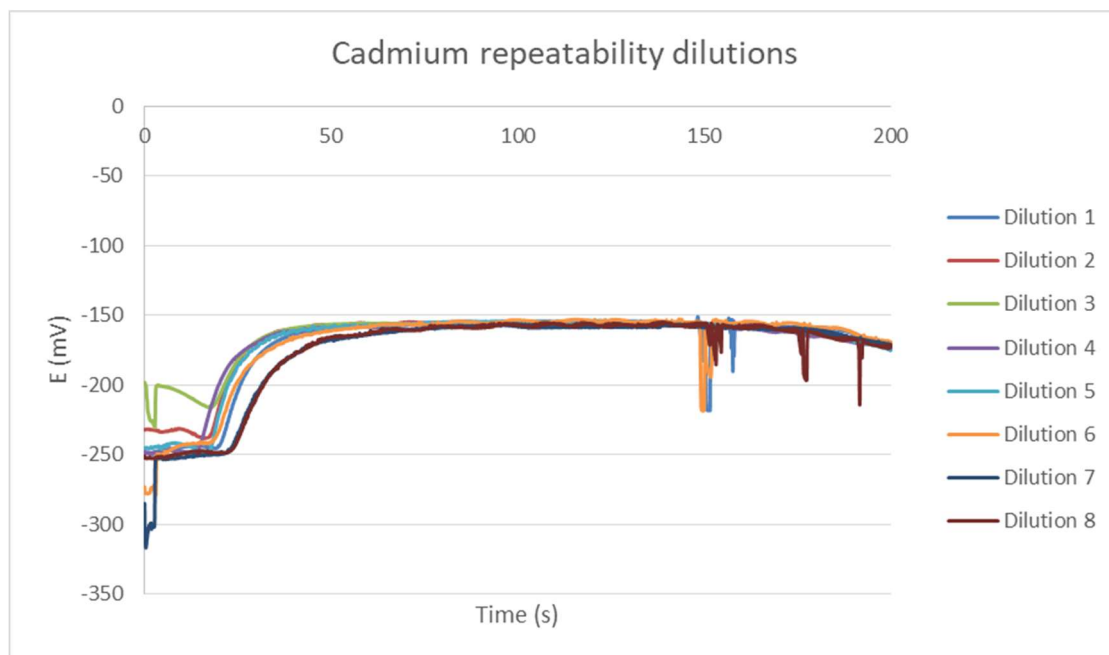


Figure 6.10 Cadmium repeatability dilutions.

The theoretical dilution made was $2,5 \cdot 10^{-3}$ M concentrated, which is -2,6 when converted to Log_{10} (C). The potential values obtained in the repeated consecutive dilutions (Figure 6.10) were converted to Log_{10} (C) in order to compare the experimental values in front of the theoretical expected (Table 6.12).

Table 6.12 Cadmium consecutive dilutions concentration.

Theo. conc. value	Experimental concentration values (expressed as Log_{10} C)								Cal. curve
	1	2	3	4	5	6	7	8	
-2,60	-2,75	-2,75	-2,75	-2,79	-2,79	-2,75	-2,86	-2,82	Initial
	-2,74	-2,74	-2,74	-2,78	-2,78	-2,74	-2,85	-2,81	Final
MOE (%)	-6	-6	-6	-7	-7	-6	-10	-9	Initial
	-5	-5	-5	-7	-7	-5	-10	-8	Final

As can be seen in the previous table, the MOE results are very low. This means that the similitude between the expected concentration value and the one determined within the system is very high.

This comparison shows that the dilution system worked as expected, that the dilutions were mixed with a high precision and that the MOEs calculated are very low.

6.4.3. Cadmium calibration without cleaning

The calibration of cadmium without cleaning was performed successfully. The results obtained are shown in the table Table 6.14.

Table 6.13 Calibration without cleaning potential.

Log C	E(mV)
-5	-222
-5	-221
-5	-222
-4	-193
-4	-192
-4	-192
-3	-163
-3	-163
-3	-163
-2	-135
-2	-134
-2	-133

Results obtained were used to calculate a calibration curve with three repetitions for every solution analysed.

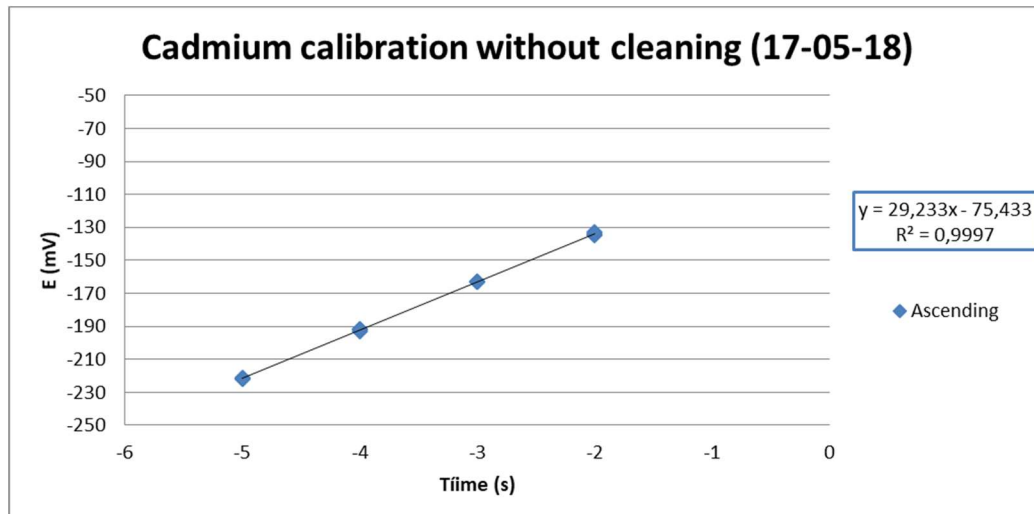


Figure 6.11 Cadmium calibration without cleaning.

In order to determine the accuracy of the calibration curve, the results obtained were compared to the acceptance criteria. The evaluation of the parameters is shown in the Table 6.14.

Table 6.14 Cadmium calibration without cleaning evaluation.

Acceptance criteria	Requirement	Performance	Results
Linearity	$0.990 < X$	0,999	✓
MEO	10 %	1,2 %	✓
Stability	$X < 0,5 \text{ mV / min}$	0,9 mV / min	✗

As it can be observed, the results obtained in the calibration were very good. The linearity was very high, the MEO was very low and the stability of the system for this determinations was the best obtained among all the internal calibrations, despite being superior to the acceptance criteria. As stated above, the stability acceptance criteria was established too low for internal calibrations with the SIA system.

Finally, it has to be taken into account that the high accuracy of the results is influenced by the robustness of the data used. In this calibration, three values were used for each concentration point instead of one.

6.5. Cesium external calibration

The conventional electrodes were calibrated externally in the pH-meter and the data were recorded (Table 6.15).

Table 6.15 Cesium external calibration.

Concentration added (M)	Volume added (μl)	Total Volume (ml)	Concentration (M)	log C	E C1 (mV)	E C2 (mV)
0	0	20	0	-5	5,5	-68,2
0,1	25	20,025	2,49E-04	-3,603	32,4	16,3
0,1	50	20,075	7,44E-04	-3,128	51,6	47,1
0,1	100	20,175	1,72E-03	-2,764	68,5	69,8
0,1	250	20,425	4,08E-03	-2,39	87,7	92,3
0,1	500	20,925	8,47E-03	-2,072	105	111
0,1	1000	21,925	1,61E-02	-1,792	121,3	128,4

With the results obtained, the calibration curve was calculated and the accuracy of the electrodes for the potential determination evaluated (Figure 6.12).

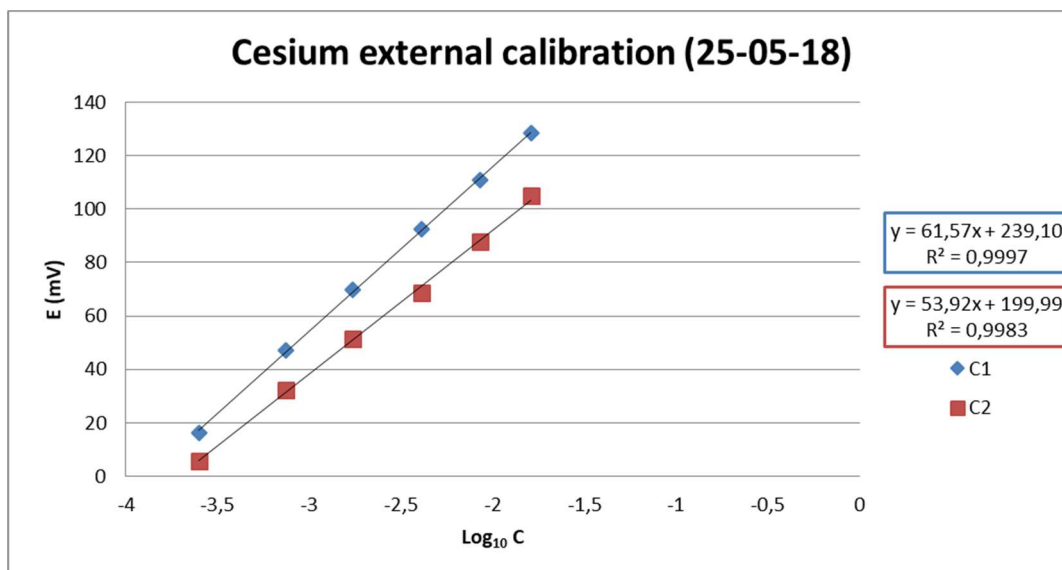


Figure 6.12 Cesium external calibration.

As explained in the section 6.1, margin of error (MEO) was calculated comparing the expected slope against the experimentally obtained.

The slope obtained is to be compared with the theoretical to obtain the Margin of Error (MEO) in percentage.

$$MEO = \frac{\text{Experimental slope}}{59,16} \times 100 \quad \text{Eq. 6.6}$$

The results of the calibration curves obtained were evaluated in respect to the acceptance criteria (Table 5.1).

Table 6.16 Cesium external calibration results.

Acceptance criteria	Requirement	Performance C1	Results	Performance C2	Results
Linearity	$0.990 < X$	0,999	✓	0,998	✓
MEO	10 %	4,1 %	✓	8,8 %	✓
Stability	$X < 0,5 \text{ mV / min}$	0,3 mV / min	✓	0,6 mV / min	✗

As it can be seen, the results obtained were very accurate in terms of linearity and margin of error. The values obtained in these two parameters were as good as the ones obtained with commercial ISEs for other heavy metals.

The stability of the electrodes was higher compared to other conventional electrodes tested. The oscillation of both electrodes was low, similar to the one obtained with commercial electrodes. Oscillations were smaller in electrode C1 than in C2, therefore the stability of the cesium electrode C1 was better than C2 and fulfilled the acceptance criteria. Generally, the performance of the electrode C1 was better than the C2.

Generally, both electrodes behaved as expected and so, their construction was considered successful.

6.6. Cesium internal calibration

The cesium calibration generated much oscillation (Figure 6.13). Nevertheless, the average value of the potential for each concentration could be calculated.

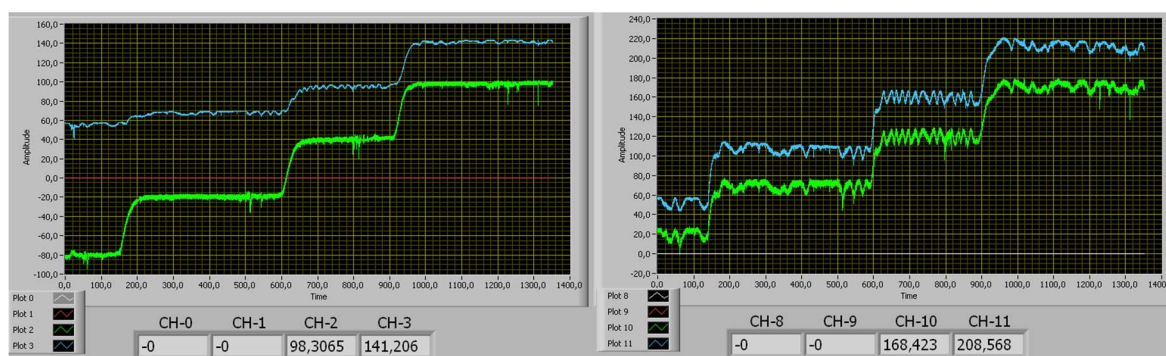


Figure 6.13 Cesium internal calibration (left: conventional electrodes; right: tubular electrodes).

The values obtained from the four electrodes were recorded.

Table 6.17 Cadmium ISEs internal calibration.

C (M)	Log C	C1 (mV)	C2 (mV)	T1 (mV)	T2 (mV)
0,00001	-5	-80	55	50	20
0,0001	-4	-20	68	110	70
0,001	-3	40	94	160	120
0,01	-2	97	140	210	170

The internal calibration of the four cesium electrodes (two conventional and two tubular electrodes) was performed and the values obtained can be observed in the figure below. The four calibration curves, generated by each of the electrodes connected to the equipment, were calculated.

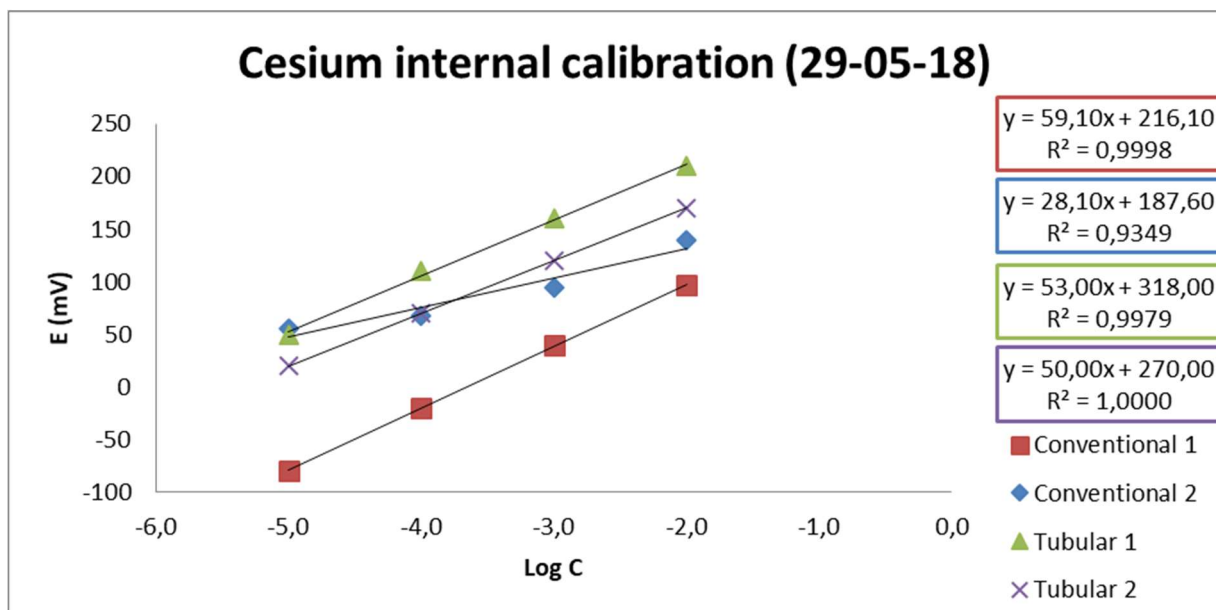


Figure 6.14 Cesium internal calibration results.

The calibration results obtained was evaluated in front of the acceptance criteria.

Table 6.18 Cesium internal calibration evaluation of the conventional electrodes.

Acceptance criteria	Requirement	Performance C1	Results	Performance C2	Results
Linearity	$0.990 < X$	0,999	✓	0,935	✗
MEO	10 %	0,1 %	✓	52,5 %	✗
Stability	$X < 0,5 \text{ mV / min}$	5 mV / min	✗	10 mV / min	✗

Table 6.19 Cesium internal calibration evaluation of the tubular electrodes.

Acceptance criteria	Requirement	Performance T1	Results	Performance T2	Results
Linearity	$0.990 < X$	0,998	✓	0,999	✓
MEO	10 %	10,4 %	✗	15,5 %	✗
Stability	$X < 0,5 \text{ mV / min}$	15 mV / min	✗	18 mV / min	✗

Some conclusions are made from this results. Despite the oscillation observed, the electrodes responded to the solution additions and increased the potential value generated. This meant that the

electrodes were working correctly since they were responding proportionally to the solutions addition. Therefore, the average values were taken into account to calculate the calibration curves. In this context, all the electrodes failed the stability acceptance criteria. Some irregularities within the SIA equipment and the electrodes must have caused this malfunctioning. Respect the other acceptance criteria, electrode C2 measured a much deviated values, with a slope half of the expected and insufficient linearity. The linearity of the electrodes T1, T2 and C1 were very good. The latter one performed in an excellent way and fulfilled linearity and MOE despite the considerable oscillation.

6.7. Biosorption results

Three biosorption experiments were conducted in this project. In each of them, a calibration was performed previous to the biosorption-desorption.

6.7.1. 1st Cesium biosorption

Calibration: The results of the calibration before the biosorption are presented in the Figure 6.15.

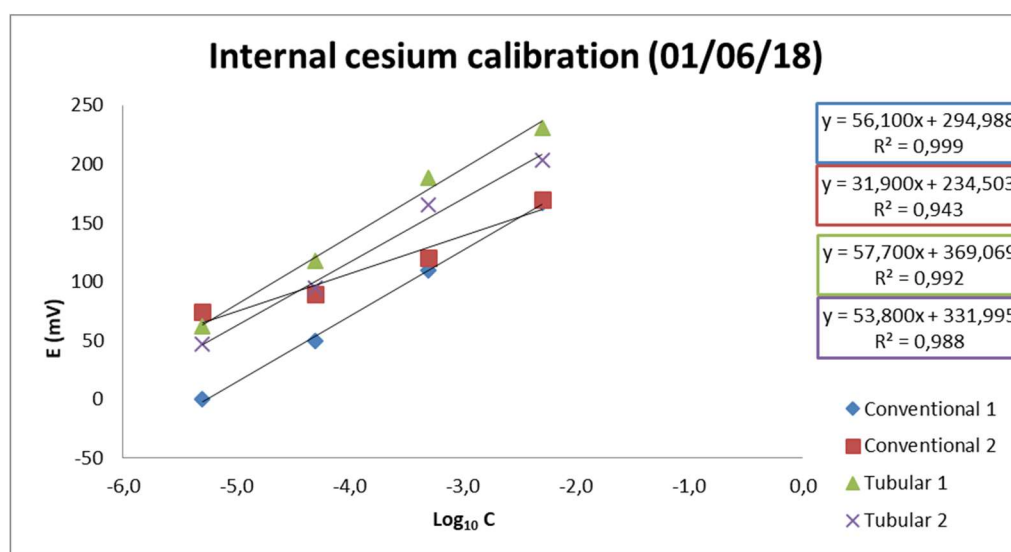


Figure 6.15 Cesium calibration before biosorption.

The values obtained for the calibration curves were analysed in front of the acceptance criteria. The goal was to determine which of the curves was more accurate, in order to take it as a reference for the biosorption. It has to be reminded that the calibration with the Cs-ISE before the biosorption was also very unstable and full of oscillations. Nevertheless, the average values could be identified and taken as a reference.

Table 6.20 Cesium biosorption calibration evaluation (1/2).

Acceptance criteria	Requirement	Performance C1	Results	Performance C2	Results
Linearity	$0.990 < X$	0,999	✓	0,943	✗
MEO	10 %	5,2 %	✓	46,1 %	✗
Stability	$X < 0,5 \text{ mV / min}$	5 mV / min	✗	9 mV / min	✗

Table 6.21 Cesium biosorption calibration evaluation (2/2).

Acceptance criteria	Requirement	Performance T1	Results	Performance T2	Results
Linearity	$0.990 < X$	0,992	✓	0,988	✗
MEO	10 %	2,5 %	✓	9,1 %	✗
Stability	$X < 0,5 \text{ mV / min}$	15 mV / min	✗	15 mV / min	✗

The results obtained in this calibration were similar to the ones obtained in the initial calibration performed to test the ISEs built. Electrodes C1 and T1 performed successfully despite the oscillation present in the equipment. On the other hand, the electrodes C2 and T2 generated a highly deviated values that did not corresponded with the theoretical values compared with the experimental values of the other two sensors.

Therefore, the electrodes C1 and T1 were taken as reference in the biosorption-desorption determination, while the other two electrodes were discarded.

Biosorption:

The results obtained during the monitoring of the biosorption process of the cesium with grape stalk are presented (Figure 6.16). Absorption experiment was executed during 115 minutes until the potential detected by the ISEs was steady. No stability was achieved during any of the calibrations, biosorptions or desorptions tests. Nevertheless, the curve obtained followed the expected behaviour. Cesium solution has to cross all the system, which is filled with an absorbent. For this reason, the detection of cesium is delayed respect other experiments. Therefore, the output solution has low content in heavy metal ions and the potential is low. After certain time, the column starts being saturated. With this, less cesium ions can be trapped by absorption in the stalk and more metal is released along with the output solution of the column. This causes that the potential measured by the electrodes is gradually increased for the presence of the heavy metal ions.

After the experiment was performed, calculations were done in order to evaluate the results obtained. Potential curves in front of time are shown in the Figure 6.16.

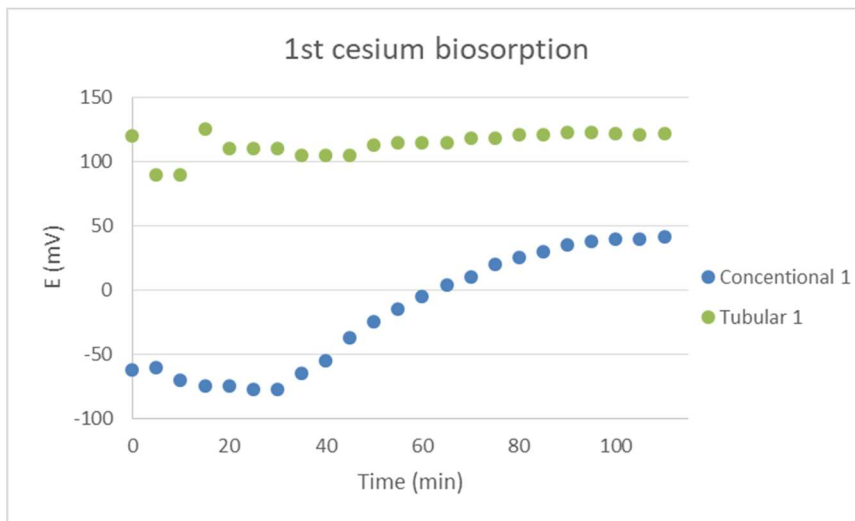


Figure 6.16 1st Cesium biosorption.

To evaluate the results obtained, the potential is converted to concentration with the calibration curves from the calibration previous to the absorption. Then, for the results analysis, the next parameters are defined:

C = concentration of the output solution at a specific moment.

C_0 = concentration of the standard solution transferred to the absorption column (70 ppm).

$$\text{Concentration ratio (\%)} = \frac{C}{C_0} \times 100 \quad \text{Eq. 6.7}$$

The results obtained are shown in the next breakthrough curve (Figure 6.17).

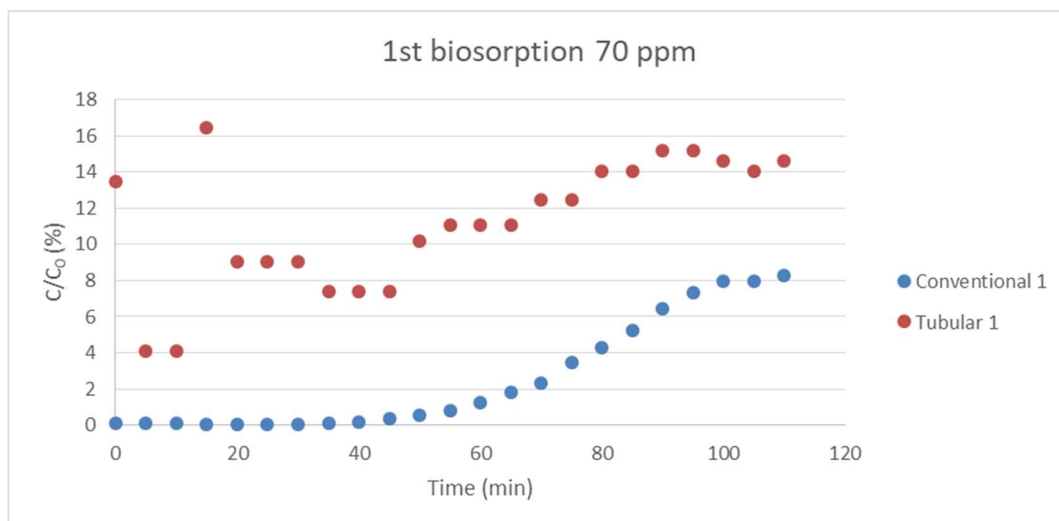


Figure 6.17 1st biosorption of 70 ppm.

As can be seen, the concentration ratio increased gradually as the grape stalk was not able to absorb all the cesium. With more time of experiment, more cesium was absorbed by the grape stalk. This means that for more time, more saturation of the stalk and less cesium retention is achieved. Therefore, the increase of the concentration ratio is an indicative of the grape stalk saturation.

After 2 hours of experiment, the signal did not increase more and hence, it was considered steady. After analysing the results, it is observed the grape was not saturated. According to the results, approximately 90% of the cesium was absorbed in the column. Nevertheless, the elapsed time was sufficient for the potential to become steady. Also, potential values returned to their expected values for such concentrations.

In this context, it is considered that the results could be caused by insufficient detection of the electrodes. They could have been worn during the process. Also, the error caused by transforming potential to concentration using the calibration curve increases the deviations due to its exponential factor.

Desorption was performed to see how much cesium was released from the grape stalk. As desorption was performed, it was used to check the error origin: the electrodes or the SIA equipment signal.

Desorption: Desorption was performed as expected and the potential curve obtained resembled the expected behaviour (see Figure 6.18). Increasing the potential initially with the release of the cesium retained in the grape stalk. Secondly, the signal diminished gradually once the grape stalk is releasing the metal and output solution is lowering its concentration. Results were recorded and analysed.

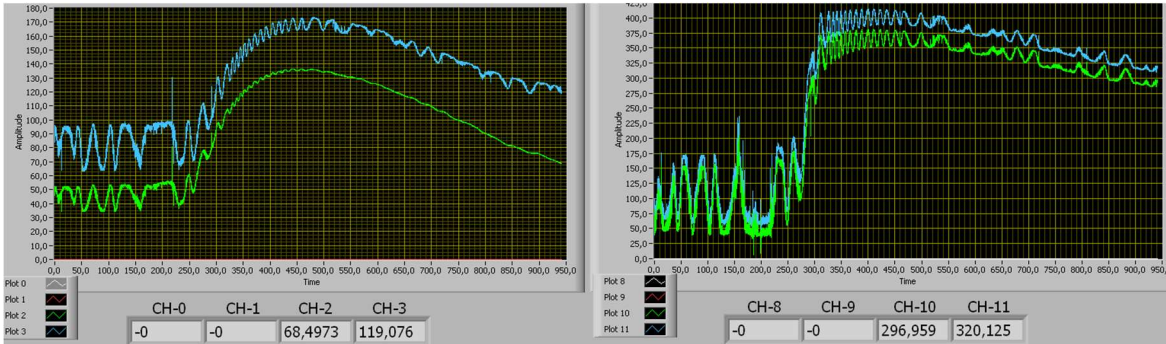


Figure 6.18 1st desorption potential.

The curve represented, potential in front time, showed a clear trend of cesium release despite the great oscillation. Then concentration of the output solution was calculated with the calibration curve equation. The results are presented in the next figure.

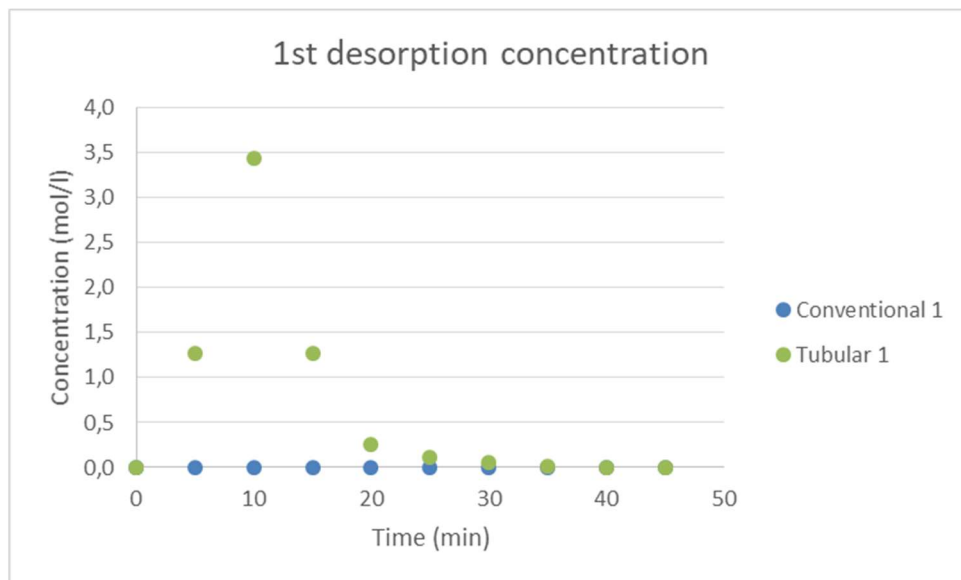


Figure 6.19 1st desorption concentration values.

As it can be observed in the figure, the concentration values determined by the tubular electrode followed the expected curve. The concentration value obtained by the conventional electrode was very low compared to the tubular electrode. Its values are considered an error and discarded for the results evaluation. The high concentration obtained by the tubular electrode suggested that cesium release from the grape stalk was sudden. The concentration of the output solution increases exponentially until reaches values higher than 3 M and then is rapidly reduced.

The tubular electrode correctly detected the desorption concentration but not in the absorption, where very low saturation values were obtained. The oscillations and bad results could be caused by different factors that reduced the signal quality such as stalk dust in the electrodes or that the

electrodes were damaged. Electrodes and system were cleaned. Then more absorptions were intended in order to obtain better results.

6.7.2. 2nd cesium biosorption

Biosorption: A second biosorption was performed and results were recorded. As it happened in previous cesium tests, high oscillations were observed during all the test. As explained above, values were converted to concentration in order to evaluate the ratio of cesium retention. Results are shown in the next figure.

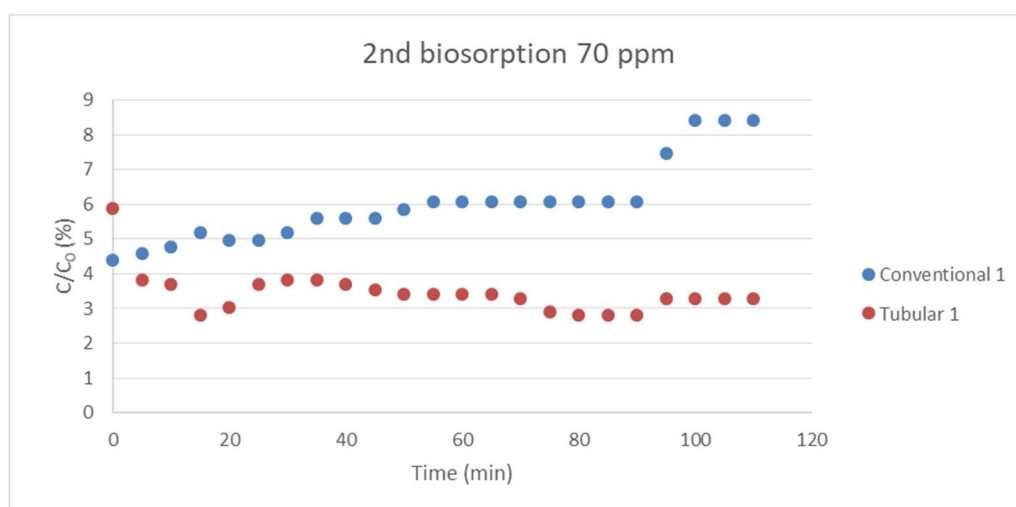


Figure 6.20 2nd biosorption of 70 ppm.

Similarly to the first biosorption, a certain expected tendency was detected. The conventional electrode increased the concentration ratio gradually as the grape stalk saturated. Nevertheless, some deviated results are obtained. Constant potential values indicate that the grape stalk was saturated, yet when converted to concentration only 10 % of the expected cesium is detected in the output solution, suggesting that the column may not be saturated.

Additionally, tubular electrode did not determine the cesium concentration in the same way than the conventional electrode. This could indicate that the electrode was damaged after the initial tests and that the latter potential detection was not successful.

As in previous absorption, desorption was executed to determine if the absorbed cesium was released.

Desorption: Desorption was successfully performed. The potential curve of the two electrodes followed the expected behaviour. Nevertheless, the concentration calculated with the respective calibration curve was lower than the one obtained in the first desorption. Considering the absorption

results obtained and the low concentration in desorption, the process was considered generally failed. It is considered that the electrodes were not determining enough potential in the absorption and desorption. Another explanation considered was that the grape stalk used was saturated and did not absorb as much cesium as expected. This idea would explain the low concentration released in the absorption but not the low concentration obtained in the absorption. Therefore, the electrodes were finally considered to be affected after the two experiments.

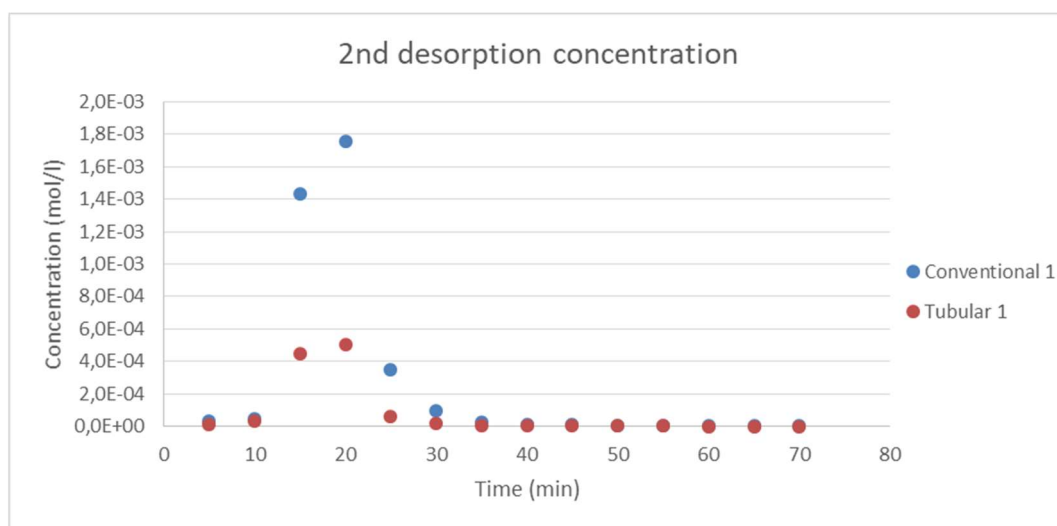


Figure 6.21 2nd desorption concentration.

After seeing the results, the system was cleaned with water in order to remove the residual acid from the absorption, to clean the electrodes and to avoid any possible source of oscillation. Latterly, a third biosorption was attempted.

6.7.3. 3rd cesium biosorption

Biosorption: The performance of the third biosorption was similar to the previous ones in the aspect of the oscillation present during all the test. The potential values initially increased indicating a cesium possible release after saturation. Latterly, the potential determined was reduced again, for an unidentified reason. This could indicate that the electrodes were not detecting correctly. The absorption results are shown in the Figure 6.22.

Considering the short-lapsed increase of potential converted to concentration ratio, it can be observed that, as in previous biosorptions, the ratio is very low and the results do not correspond with the expected theoretically. These value of ratio do not correspond to saturation, but the system behaved unsteady and the absorption was interrupted.

Finally, desorption was performed to clarify if the cesium was absorbed in the grape stalk.

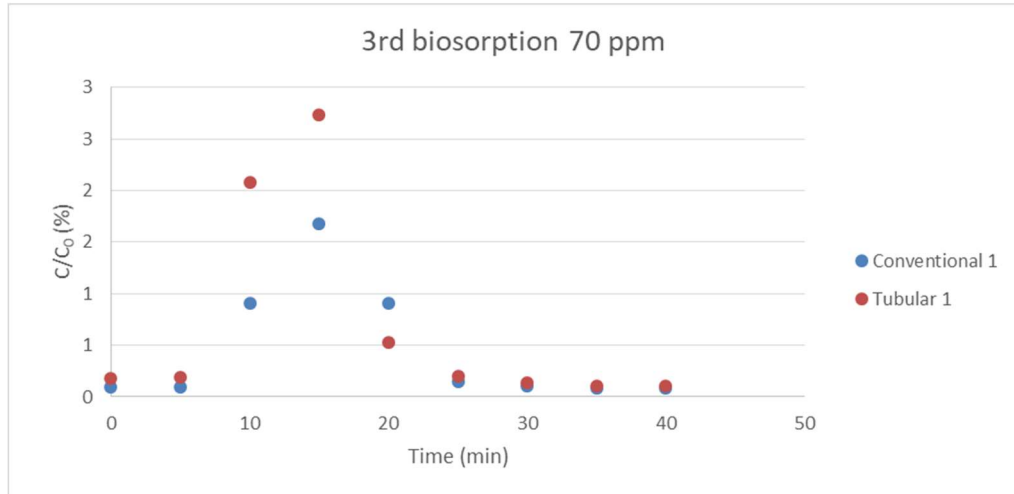


Figure 6.22 3rd biosorption of 70 ppm.

Desorption: Desorption results obtained did not coincided with previous tests. The increase of potential was not sudden and the concentrations reached were lower than in other desorptions, as if there was no cesium released from the stalk.

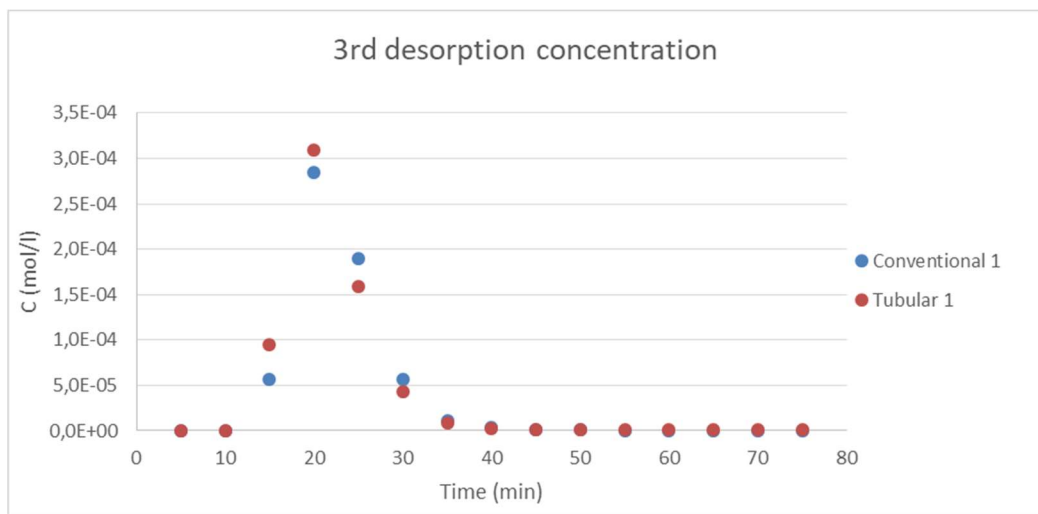


Figure 6.23 3rd desorption concentration.

7. Environmental impact analysis

In the development of this project, many standard solutions were prepared with reagents containing different metals such as copper, cadmium and cesium. The volume consumed of these solutions was approximately about one litre per week. These solutions were properly recycled in waste treatment agencies where the heavy metals were recovered.

The rest of wastes generated is related to the laboratory activity: nitrile gloves, absorbent paper and other plastic disposable items such as Pasteur pipettes, burette and so on.

On the other side, it has to be considered that the framework of this project is the improvement of detection and monitoring systems for heavy metals and other metals pollution control.

Additionally, projects like this has a great potential positive impact in the economy at long term. In case that these kind of technologies were used worldwide, the agriculture wastes generated from human activities could be reutilised for an eco-friendly solution. This would help creating circular economy by revaluing the wastes, nowadays discarded. Finally, it has to be considered that the agricultural waste itself creates great environmental problems such as eutrophication, which would be slightly reduced.

Conclusions

SIA equipment was successfully used to calibrate different ion selective electrodes. The many tests performed helped optimising the calibration methods and isolation signal noise sources. Some metals and their respective ISE were easier to calibrate and to use for tests than others.

Copper calibrations were less successful than the ones performed with cadmium. This could be caused due to a higher selectivity of the electrode used for its target ion or because of better stability of the solutions.

The capacity of the equipment to create internal dilutions from different standard solutions was proved. Introducing different standard solutions through the channel and diluting with the carrier solution through the burette was demonstrated to be useful and accurate. The great potential of this tool is to be used in ET. The possibility to mix different solutions within the equipment to create infinite different solutions. This would allow calibrating ET with a reduced equipment and a little expense of reagents.

Cesium electrodes were built successfully following the defined procedures and some electrodes responded to the cesium concentrations as expected. The cesium electrodes could be tested in the SIA system and calibrated.

The online connection of the equipment with the NIVA-RAdB was studied. The transmission of successful concentration determination was not achieved. Nevertheless, the definition of the characteristics for the data transmission was done.

Economic analysis

In this section of the project, the costs of the development of this project are considered, including costs of equipment, energy, personnel and reagents. The calculation of the costs is an approximation, therefore, the results are rounded to the unity, with no decimals.

Personnel

The hours spent in the development of this project by the author of this thesis are considered as a junior engineer. The additional advice and guidance received from other researchers is counted as senior engineer salary. Additionally, the help received from computer technicians for programs improvements is considered.

Table 0.1 Personnel costs.

Personnel	Salary (€/h)	Hours of work (h)	Total expense (€)
Junior engineer	20	500	10.000
Senior engineer	50	50	2.500
Computer technician	45	20	900
		Total	13.400 €

Equipment

The new control computer was the only new equipment purchased specifically for the realisation of this project. The rest of the equipment costs are considered as an amortization of its initial costs during the development of this project. The amortization is calculated according the next equation.

$$\textit{Amortization} = \frac{\textit{Purchase cost}}{\textit{Shelf life}} \times \textit{Period of utilisation} \quad \text{Eq. 0.1}$$

With this, the costs of utilisation of the all the equipment are calculated. Some equipment have lasted more than their expected shelf life. Those equipment have not been considered for the costs calculations because they have been totally amortized.

Table 0.2 Equipment costs.

Equipment	Purchase cost (€)	Shelf life (years)	Period of utilisation (years)	Amortization (€)
Copper ISE	780	10	0.5	39
Cadmium ISE	880	10	0.5	44
SIA equipment	27200	10	0.5	1360
New computer	1099	6	0.1	18
pH-meter	920	10	0.5	46
			Total	1465 €

Laboratory materials and reagents

The costs of the reagents and materials is multiplied for the number of units used or consumed. The updated costs of the reagents was obtained from the Merck catalogue [53]. These costs represent a worst case, including all the reagents used, despite in many cases the amount of reagent consumed was lower than the unit.

Table 0.3 Reagents and materials costs.

Material	Purchase cost (€)	Units	Total cost (€)
Nitrile globe	4,00	1 box	4
Beaker	23,25	5	117
Volumetric flask	3,15	8	25
Waste management	3,50	1	4
Potassium nitrate	4,99	1	5
Copper nitrate	44,25	1	44
Cadmium nitrate	58	1	58
Cesium nitrate	100	1	100
TRIS	93,50	1	94
Nitric acid	143,50	1	144
		Total	595 €

Additionally, a total expense of 100 € is calculated approximately as water and power supplies cost.

Total costs

The total amount of expenses for this project are summarized in the next table.

Table 0.4 Total expenses.

Concept	Cost (€)
Personnel	13.400
Equipment	1465
Materials and reagents	595
Supplies	100
Pre-tax expenses	15.560
Taxes (21 %)	3268
TOTAL	18.828 €

The total cost of the project is 18.828 €.

Future research

Future research can be approached from several aspects of this project. Some general ideas are exposed here:

- To complete the program modification for online connection. This task will take a considerable amount of work for itself on learning programming, SFTP programming and Labview modification for data transmission. If the communication of the equipment is achieved, trials should be carried for generating more data in a continuation of the collaboration with the NIVA institute.
- Generation of an Electronic Tongue and train inside the SIA. Current investigations show that it is feasible to use the ET technology to detect multimetal solutions. The goal of the SIA equipment is to create a fast, simple method for ET training, therefore, a good final stage for the equipment would be to create an ET internally and trained within the SIA system.
- If an ET is built, multimetal biosorptions could be performed in order to widen the knowledge of how is the kinetics of the biosorptions, which biomaterials are more suited for biosorption among other subjects to be investigated. Additionally, biosorption could be tested within the SIA conduits.
- Improvement of calibrations and stabilisation of the equipment. When executing tests in future works, the observations made in this project should be taken into account. Cadmium electrode and solutions were easier to work with, which makes them good candidates for equipment testing. On the other hand, improvement of the determinations performed with the other metals could be considered.
- To treat the determinations statistically to improve the robustness of the results, increasing thus the knowledge obtained from experiments. Many variations could be made such as: considering the surface under the curves instead of maximum values in the potential determinations. To study the differences between repeated dilutions to detect possible equipment deviations among others.
- For further works, it was considered that a way to perform the modification of the data files would be with an automatic program or script that converted the potential values in concentration with the most recent calibration curve. With that, the values generated would be heavy metal concentration instead of potential. Additionally, this program could store the data differently, by only processing those data fields different than 0.0000 mV.

Bibliography

- [1] R. Haunschild, L. Bornmann, and W. Marx, "Climate Change Research in View of Bibliometrics," *PLoS One*, vol. 11, no. 7, p. e0160393, 2016.
- [2] M. Ahsan *et al.*, "Heavy metal accumulation imparts structural differences in fragrant *Rosa* species irrigated with marginal quality water," *Ecotoxicol. Environ. Saf.*, vol. 159, pp. 240–248, 2018.
- [3] G. W. Bryan and W. J. Langston, "Bioavailability, accumulation and effects of heavy metals in sediments with special reference to United Kingdom estuaries: a review," *Environ. Pollut.*, vol. 76, no. 2, pp. 89–131, 1992.
- [4] N. Dorey, S. Martin, F. Oberhänsli, J.-L. Teyssié, R. Jeffree, and T. Lacoue-Labarthe, "Ocean acidification modulates the incorporation of radio-labeled heavy metals in the larvae of the Mediterranean sea urchin *Paracentrotus lividus*," *J. Environ. Radioact.*, vol. 190–191, pp. 20–30, Oct. 2018.
- [5] L. Järup, "Hazards of heavy metal contamination," *British Medical Bulletin*. 2003.
- [6] P. B. Tchounwou, C. G. Yedjou, A. K. Patlolla, and D. J. Sutton, "Heavy Metal Toxicity and the Environment," Springer, Basel, 2012, pp. 133–164.
- [7] W. J. Langston, "Toxic Effects of Metals and the Incidence of Metal Pollution in Marine Ecosystems," pp. 101–120, Jan. 2018.
- [8] D. Wilson, M. Del Valle, S. Alegret, C. Valderrama, and A. Florido, "Simultaneous and automated monitoring of the multimetal biosorption processes by potentiometric sensor array and artificial neural network," *Talanta*, 2013.
- [9] D. Wilson, M. Del Valle, S. Alegret, C. Valderrama, and A. Florido, "Potentiometric electronic tongue-flow injection analysis system for the monitoring of heavy metal biosorption processes," *Talanta*, 2012.
- [10] A. Florido, C. Valderrama, S. Nualart, L. Velazco-Molina, A. A. de Fuentes, and M. del Valle, "Computer controlled-flow injection potentiometric system based on virtual instrumentation for the monitoring of metal-biosorption processes," *Anal. Chim. Acta*, 2010.
- [11] C. Solis, "Implementation and optimization of a sequential injection analysis (SIA) system by UV-Visible spectroscopy." UPC, Barcelona, p. 75, 2016.
- [12] J. L. Núñez, "Estudio de la fluidica asociada a la optimización de un sistema de análisis por inyección secuencial (SIA)." 2016.
- [13] H. Sánchez, "Implementación y optimización de un sistema de análisis por inyección secuencial (SIA) totalmente automatizado basado en sensores potenciométricos," 2017.
- [14] D. Fandos, "Elaboración de un sensor de cesio. Aplicación en biosorción con raspo de uva." p.

90, 2016.

- [15] A. Rojo, "Evaluación de sensores convencionales para la determinación de diferentes iones en la biosorción mediante un residuo vegetal." p. 111, 2017.
- [16] Ş. Tokalioğlu, Ş. Kartal, and L. Elçi, "Determination of heavy metals and their speciation in lake sediments by flame atomic absorption spectrometry after a four-stage sequential extraction procedure," *Anal. Chim. Acta*, vol. 413, no. 1–2, pp. 33–40, May 2000.
- [17] M. Faraji, Y. Yamini, A. Saleh, M. Rezaee, M. Ghambarian, and R. Hassani, "A nanoparticle-based solid-phase extraction procedure followed by flow injection inductively coupled plasma-optical emission spectrometry to determine some heavy metal ions in water samples," *Anal. Chim. Acta*, vol. 659, no. 1–2, pp. 172–177, Feb. 2010.
- [18] C. R. T. Tarley, V. S. Santos, B. E. L. Baêta, A. C. Pereira, and L. T. Kubota, "Simultaneous determination of zinc, cadmium and lead in environmental water samples by potentiometric stripping analysis (PSA) using multiwalled carbon nanotube electrode," *J. Hazard. Mater.*, vol. 169, no. 1–3, pp. 256–262, Sep. 2009.
- [19] Y. Umezawa, P. Bühlmann, K. Umezawa, K. Tohda, and S. Amemiya, "Potentiometric Selectivity Coefficients of Ion-Selective Electrodes. Part I. Inorganic Cations (Technical Report)," *Pure Appl. Chem.*, vol. 72, no. 10, pp. 1851–2082, Jan. 2000.
- [20] V. K. Gupta, M. R. Ganjali, P. Norouzi, H. Khani, A. Nayak, and S. Agarwal, "Electrochemical Analysis of Some Toxic Metals by Ion-Selective Electrodes," *Crit. Rev. Anal. Chem.*, vol. 41, no. 4, pp. 282–313, Oct. 2011.
- [21] E. Y. Z. Frag, T. A. Ali, G. G. Mohamed, and Y. H. H. Awad, "Construction of Different Types of Ion-Selective Electrodes. Characteristic Performances and Validation for Direct Potentiometric Determination of Orphenadrine Citrate," *Int. J. Electrochem. Sci.*, vol. 7, pp. 4443–4464, 2012.
- [22] E. Bakker and E. Pretsch, "Peer Reviewed: The New Wave of Ion-Selective Electrodes," *Anal. Chem.*, vol. 74, no. 15, p. 420 A-426 A, 2002.
- [23] † John J. Lavigne *et al.*, "Solution-Based Analysis of Multiple Analytes by a Sensor Array: Toward the Development of an 'Electronic Tongue,'" 1998.
- [24] F. Winquist, J. Olsson, and M. Eriksson, "Multicomponent analysis of drinking water by a voltammetric electronic tongue," *Anal. Chim. Acta*, vol. 683, no. 2, pp. 192–197, Jan. 2011.
- [25] G. De Vera, M. A. Climent, C. Antón, A. Hidalgo, and C. Andrade, "Determination of the selectivity coefficient of a chloride ion selective electrode in alkaline media simulating the cement paste pore solution."
- [26] G. D. Christian, "Flow analysis and its role and importance in the analytical sciences," in *Analytica Chimica Acta*, 2003.
- [27] V. Cerdà and J. M. Estela, "Injection Techniques in Flow Analysis," in *Advances in Flow Analysis*, 2008.

- [28] R. B. R. Mesquita and A. O. S. S. Rangel, "A review on sequential injection methods for water analysis," *Anal. Chim. Acta*, 2009.
- [29] A. Gutés, "Llengües electròniques voltamperomètriques, Tesis Doctoral, UAB," 2006.
- [30] F. Fu and Q. Wang, "Removal of heavy metal ions from wastewaters: A review," *J. Environ. Manage.*, vol. 92, no. 3, pp. 407–418, Mar. 2011.
- [31] M. A. Hashim, S. Mukhopadhyay, J. N. Sahu, and B. Sengupta, "Remediation technologies for heavy metal contaminated groundwater," *J. Environ. Manage.*, vol. 92, no. 10, pp. 2355–2388, Oct. 2011.
- [32] R. M. Atlas and T. C. Hazen, "Oil Biodegradation and Bioremediation: A Tale of the Two Worst Spills in U.S. History," *Environ. Sci. Technol.*, vol. 45, no. 16, pp. 6709–6715, Aug. 2011.
- [33] J. He and J. P. Chen, "A comprehensive review on biosorption of heavy metals by algal biomass: Materials, performances, chemistry, and modeling simulation tools," *Bioresour. Technol.*, vol. 160, pp. 67–78, May 2014.
- [34] N. Feng, X. Guo, S. Liang, Y. Zhu, and J. Liu, "Biosorption of heavy metals from aqueous solutions by chemically modified orange peel," *J. Hazard. Mater.*, vol. 185, no. 1, pp. 49–54, Jan. 2011.
- [35] A. Witek-Krowiak, R. G. Szafran, and S. Modelski, "Biosorption of heavy metals from aqueous solutions onto peanut shell as a low-cost biosorbent," *Desalination*, vol. 265, no. 1–3, pp. 126–134, Jan. 2011.
- [36] G. Blázquez, M. A. Martín-Lara, G. Tenorio, and M. Calero, "Batch biosorption of lead(II) from aqueous solutions by olive tree pruning waste: Equilibrium, kinetics and thermodynamic study," *Chem. Eng. J.*, vol. 168, no. 1, pp. 170–177, Mar. 2011.
- [37] C. Valderrama, J. A. Arévalo, I. Casas, M. Martínez, N. Miralles, and A. Florido, "Modelling of the Ni(II) removal from aqueous solutions onto grape stalk wastes in fixed-bed column," *J. Hazard. Mater.*, vol. 174, no. 1–3, pp. 144–150, Feb. 2010.
- [38] A. Florido, C. Valderrama, J. A. Arévalo, I. Casas, M. Martínez, and N. Miralles, "Application of two sites non-equilibrium sorption model for the removal of Cu(II) onto grape stalk wastes in a fixed-bed column," *Chem. Eng. J.*, vol. 156, no. 2, pp. 298–304, Jan. 2010.
- [39] N. Miralles, C. Valderrama, I. Casas, M. Martínez, and A. Florido, "Cadmium and Lead Removal from Aqueous Solution by Grape Stalk Wastes: Modeling of a Fixed-Bed Column," *J. Chem. Eng. Data*, vol. 55, no. 9, pp. 3548–3554, Sep. 2010.
- [40] C. Escudero, J. Poch, and I. Villaescusa, "Modelling of breakthrough curves of single and binary mixtures of Cu(II), Cd(II), Ni(II) and Pb(II) sorption onto grape stalks waste," *Chem. Eng. J.*, vol. 217, pp. 129–138, Feb. 2013.
- [41] K. E. Tollefsen, "RADB - NIVA." [Online]. Available: <https://www.niva.no/en/projectweb/radb>. [Accessed: 12-May-2018].

- [42] P. García, "Optimización de un sistema de análisis por inyección secuencial (SIA) multisensor totalmente automatizado." p. 105, 2018.
- [43] Y. Choi, H. Kim, J. K. Lee, S. H. Lee, H. Bin Lim, and J. S. Kim, "Cesium ion-selective electrodes based on 1,3-alternate thiacalix[4]biscrown-6,6,," *Talanta*, vol. 64, no. 4, pp. 975–80, Nov. 2004.
- [44] S. Ghorbanzadeh Mashkani and P. Tajer Mohammad Ghazvini, "Biotechnological potential of *Azolla filiculoides* for biosorption of Cs and Sr: Application of micro-PIXE for measurement of biosorption," *Bioresour. Technol.*, vol. 100, no. 6, pp. 1915–1921, Mar. 2009.
- [45] A. E. Ofomaja, A. Pholosi, and E. B. Naidoo, "Kinetics and competitive modeling of cesium biosorption onto chemically modified pine cone powder," *J. Taiwan Inst. Chem. Eng.*, vol. 44, no. 6, pp. 943–951, Nov. 2013.
- [46] H. Parab and M. Sudersanan, "Engineering a lignocellulosic biosorbent – Coir pith for removal of cesium from aqueous solutions: Equilibrium and kinetic studies," *Water Res.*, vol. 44, no. 3, pp. 854–860, Feb. 2010.
- [47] D. International Association on Water Pollution Research. *et al.*, *Water research*. Elsevier, 2013.
- [48] D. Chakraborty, S. Maji, A. Bandyopadhyay, and S. Basu, "Biosorption of cesium-137 and strontium-90 by mucilaginous seeds of *Ocimum basilicum*," *Bioresour. Technol.*, vol. 98, no. 15, pp. 2949–2952, Nov. 2007.
- [49] B. Pangen, H. Paudyal, K. Inoue, K. Ohto, H. Kawakita, and S. Alam, "Preparation of natural cation exchanger from persimmon waste and its application for the removal of cesium from water," *Chem. Eng. J.*, vol. 242, pp. 109–116, Apr. 2014.
- [50] C. Chen and J. Wang, "Removal of Pb²⁺, Ag⁺, Cs⁺ and Sr²⁺ from aqueous solution by brewery's waste biomass," *J. Hazard. Mater.*, vol. 151, no. 1, pp. 65–70, Feb. 2008.
- [51] M. . Balarama Krishna, S. . Rao, J. Arunachalam, M. . Murali, S. Kumar, and V. . Manchanda, "Removal of ¹³⁷Cs and ⁹⁰Sr from actual low level radioactive waste solutions using moss as a phyto-sorbent," *Sep. Purif. Technol.*, vol. 38, no. 2, pp. 149–161, Aug. 2004.
- [52] Y. Z. Ding, @bullet Z G Song, @bullet R W Feng, and @bullet J K Guo, "Interaction of organic acids and pH on multi-heavy metal extraction from alkaline and acid mine soils."
- [53] "Spain | Sigma-Aldrich." [Online]. Available: <https://www.sigmaaldrich.com/spain.html>. [Accessed: 15-Jun-2018].

Index of figures

Figure 3.1 Standard FIA system [27].	11
Figure 3.2 Standard SIA system [29].	12
Figure 3.3 Overview of NIVA RAdb operating mechanism [41].	14
Figure 4.1 SIA system in the EEBE laboratory [42].	17
Figure 4.2 SIA system diagram [12].	18
Figure 4.3 Example of dilution with the diluent through reagent channels [12].	19
Figure 4.4 Data recorded by Labview in .txt format.	21
Figure 5.1 External calibration [42].	24
Figure 5.3 Ionophore thicalix[4]-bis(crown-6) [43].	30
Figure 5.4 Electrode mixture deposition in conventional electrodes.	31
Figure 5.5 Tubular electrodes.	32
Figure 5.6 Cesium failed internal calibration.	34
Figure 5.7 Cesium ISEs calibration.	35
Figure 5.8 Absorption column purge.	37
Figure 5.9 Cesium biosorption setup.	38
Figure 5.10 System manifold.	39
Figure 5.11 Bubble trap.	40

Figure 5.12 ISE dilution space.	41
Figure 5.13 45° ISE positioning [42].	42
Figure 5.14 Channels deviation checking.	43
Figure 5.15 $[\text{Cu}^{2+}] = 10^{-5} \text{ M}$ and $[\text{Cu}^{2+}] = 10^{-3} \text{ M}$ equilibrium chart.	45
Figure 5.16 $[\text{Cu}^{2+}] = 10^{-1} \text{ M}$ equilibrium chart.	45
Figure 5.17 Test file for SFTP.	49
Figure 6.1 Copper external calibration.	50
Figure 6.2 Copper internal calibration.	52
Figure 6.3 Copper internal calibration.	53
Figure 6.4 Copper repeatability calibration.	54
Figure 6.5 Copper dilutions repeatability.	56
Figure 6.6 Cadmium external calibration.	57
Figure 6.7 Cadmium internal calibration.	58
Figure 6.8 Cadmium internal calibration.	59
Figure 6.9 Cadmium repeatability calibration.	60
Figure 6.10 Cadmium repeatability dilutions.	62
Figure 6.11 Cadmium calibration without cleaning.	63
Figure 6.12 Cesium external calibration.	65
Figure 6.13 Cesium internal calibration (left: conventional electrodes; right: tubular electrodes).	66

Figure 6.14 Cesium internal calibration results.	67
Figure 6.15 Cesium calibration before biosorption.	68
Figure 6.16 1 st Cesium biosorption.	70
Figure 6.17 1st biosorption of 70 ppm.	71
Figure 6.18 1st desorption potential.	72
Figure 6.19 1st desorption concentration values.	72
Figure 6.20 2nd biosorption of 70 ppm.	73
Figure 6.21 2nd desorption concentration.	74
Figure 6.22 3rd biosorption of 70 ppm.	75
Figure 6.23 3rd desorption concentration.	75
Figure 0.1 Data acquisition card datasheet.	98

Index of tables

Table 5.1 Acceptance criteria.	22
Table 5.2 $\text{Cu}(\text{NO}_3)_2$ standard solutions.	23
Table 5.3 Copper external calibration.	24
Table 5.4 $\text{Cd}(\text{NO}_3)_2$ standard solutions	27
Table 5.5 Mixture composition [43].	31
Table 5.6 $\text{Cs}(\text{NO}_3)$ standard solutions.	33
Table 5.7 Absorption capacity of different biomass [14].	36
Table 6.1 Copper external calibration results.	50
Table 6.2 Copper external calibration performance.	51
Table 6.3 Copper internal calibration.	52
Table 6.4 Copper internal calibration performance.	53
The Table 6.5 Copper repeatability calibration.	55
Table 6.6 Copper consecutive dilutions concentration.	56
Table 6.7 Cadmium external calibration.	57
Table 6.8 Cadmium external calibration performance.	58
Table 6.9 Cadmium internal calibration.	59
Table 6.10 Cadmium internal calibration performance.	59

Table 6.11 Cadmium repeatability calibration. _____	61
Table 6.12 Cadmium consecutive dilutions concentration. _____	62
Table 6.13 Calibration without cleaning potential. _____	63
Table 6.14 Cadmium calibration without cleaning evaluation. _____	64
Table 6.15 Cesium external calibration. _____	64
Table 6.16 Cesium external calibration results. _____	65
Table 6.17 Cadmium ISEs internal calibration. _____	66
Table 6.18 Cesium internal calibration evaluation of the conventional electrodes. _____	67
Table 6.19 Cesium internal calibration evaluation of the tubular electrodes. _____	67
Table 6.20 Cesium biosorption calibration evaluation (1/2). _____	69
Table 6.21 Cesium biosorption calibration evaluation (2/2). _____	69
Table 0.1 Personnel costs. _____	79
Table 0.2 Equipment costs. _____	80
Table 0.3 Reagents and materials costs. _____	80
Table 0.4 Total expenses. _____	81

Index of equations

Eq. 3.1	7
Eq. 3.2	8
Eq. 3.3	8
Eq. 3.4	8
Eq. 3.5	8
Eq. 3.6	8
Eq. 3.7	8
Eq. 3.8	8
Eq. 4.1	20
Eq. 5.1	26
Eq. 6.1	51
Eq. 6.2	55
Eq. 6.3	55
Eq. 6.4	61
Eq. 6.5	61
Eq. 6.6	65
Eq. 6.7	70

Eq. 0.1

79

Annex A. Scripts

In this annexe, different scripts are described as an example.

Annexe A.1 - Acquisition script 2 hours

4,P100T7200:

Annexe A.2 – Channels and electrodes cleaning

2,IE21V20.P40000.:	Aspire 5 ml
1,10:	Open valve 1
2,OE20V50.D20000.:	Dispense 2.5ml
1,100:	Open valve 2
2,OE20V50.D20000.:	Dispense 2.5ml
2,IE21V20.P40000.:	Dispense 5ml
1,1000:	Open valve 3
2,OE20V50.D20000.:	Dispense 2.5ml
1,10000:	Open valve 4
2,OE20V50.D20000.:	Dispense 2.5ml
2,IE21V50.P40000.:	Aspire 5ml
1,1000000:	Open valve 6
2,OE20V50.D40000.:	Dispense 5ml
1,0:	Close all valves

Annexe A.3 – Calibration with 4 cleaning stages

2,IE21V20.D40000.:	Empty
2,IE21V25.P40000.:	Aspire for cleaning 1
2,OE20V25.D40000.:	Dispense for cleaning 1
1,10:	Open valve 1
2,OE20V150.P40000.:	Aspire reagent 1
1,1000000:	Open valve 6
4,P100T6000:	Start acquisition 1h 40 min
2,OE20V250.D40000.:	Send reagent
1,1000000:	Open valve 6
2,IE21V25.P40000.:	Aspire for cleaning 1
2,OE20V25.D40000.:	Dispense for cleaning 1
2,IE21V25.P40000.:	Aspire for cleaning 2
2,OE20V25.D40000.:	Dispense for cleaning 2
2,IE21V25.P40000.:	Aspire for cleaning 3
2,OE20V25.D40000.:	Dispense for cleaning 3

2,IE21V25.P40000.:	Aspire for cleaning 4
2,OE20V25.D40000.:	Dispense for cleaning 4
1,100:	Open valve 2
2,OE20V150.P40000.:	Aspire reagent 2
1,1000000:	Open valve 6
2,OE20V250.D40000.:	Send reagent
1,1000000:	Open valve 6
2,IE21V25.P40000.:	Aspire for cleaning 1
2,OE20V25.D40000.:	Dispense for cleaning 1
2,IE21V25.P40000.:	Aspire for cleaning 2
2,OE20V25.D40000.:	Dispense for cleaning 2
2,IE21V25.P40000.:	Aspire for cleaning 3
2,OE20V25.D40000.:	Dispense for cleaning 3
2,IE21V25.P40000.:	Aspire for cleaning 4
2,OE20V25.D40000.:	Dispense for cleaning 4
1,1000:	Open valve 3
2,OE20V150.P40000.:	Aspire reagent 3
1,1000000:	Open valve 6
2,OE20V250.D40000.:	Send reagent
1,1000000:	Open valve 6
2,IE21V25.P40000.:	Aspire for cleaning 1
2,OE20V25.D40000.:	Dispense for cleaning 1
2,IE21V25.P40000.:	Aspire for cleaning 2
2,OE20V25.D40000.:	Dispense for cleaning 2
2,IE21V25.P40000.:	Aspire for cleaning 3
2,OE20V25.D40000.:	Dispense for cleaning 3
2,IE21V25.P40000.:	Aspire for cleaning 4
2,OE20V25.D40000.:	Dispense for cleaning 4
1,10000:	Open valve 4
2,OE20V150.P40000.:	Aspire reagent 4
1,1000000:	Open valve 6
2,OE20V250.D40000.:	Send reagent
1,1000000:	Open valve 6
2,IE21V25.P40000.:	Aspire for cleaning 1
2,OE20V25.D40000.:	Dispense for cleaning 1
2,IE21V25.P40000.:	Aspire for cleaning 2
2,OE20V25.D40000.:	Dispense for cleaning 2
2,IE21V25.P40000.:	Aspire for cleaning 3
2,OE20V25.D40000.:	Dispense for cleaning 3
2,IE21V25.P40000.:	Aspire for cleaning 4
2,OE20V25.D40000.:	Dispense for cleaning 4

1,10000:	Open valve 4
2,OE20V150.P40000.:	Aspire reagent 4
1,1000000:	Open valve 6
2,OE20V250.D40000.:	Send reagent
1,1000000:	Open valve 6
2,IE21V25.P40000.:	Aspire for cleaning 1
2,OE20V25.D40000.:	Dispense for cleaning 1
2,IE21V25.P40000.:	Aspire for cleaning 2
2,OE20V25.D40000.:	Dispense for cleaning 2
2,IE21V25.P40000.:	Aspire for cleaning 3
2,OE20V25.D40000.:	Dispense for cleaning 3
2,IE21V25.P40000.:	Aspire for cleaning 4
2,OE20V25.D40000.:	Dispense for cleaning 4
1,1000:	Open valve 3
2,OE20V150.P40000.:	Aspire reagent 3
1,1000000:	Open valve 6
2,OE20V250.D40000.:	Send reagent
1,1000000:	Open valve 6
2,IE21V25.P40000.:	Aspire for cleaning 1
2,OE20V25.D40000.:	Dispense for cleaning 1
2,IE21V25.P40000.:	Aspire for cleaning 2
2,OE20V25.D40000.:	Dispense for cleaning 2
2,IE21V25.P40000.:	Aspire for cleaning 3
2,OE20V25.D40000.:	Dispense for cleaning 3
2,IE21V25.P40000.:	Aspire for cleaning 4
2,OE20V25.D40000.:	Dispense for cleaning 4
1,100:	Open valve 2
2,OE20V150.P40000.:	Aspire reagent 2
1,1000000:	Open valve 6
2,OE20V250.D40000.:	Send reagent
1,1000000:	Open valve 6
2,IE21V25.P40000.:	Aspire for cleaning 1
2,OE20V25.D40000.:	Dispense for cleaning 1
2,IE21V25.P40000.:	Aspire for cleaning 2
2,OE20V25.D40000.:	Dispense for cleaning 2
2,IE21V25.P40000.:	Aspire for cleaning 3
2,OE20V25.D40000.:	Dispense for cleaning 3
2,IE21V25.P40000.:	Aspire for cleaning 4
2,OE20V25.D40000.:	Dispense for cleaning 4
1,10:	Open valve 1
2,OE20V150.P40000.:	Aspire reagent 1

1,1000000:	Open valve 6
2,OE20V25.D40000.:	Send reagent
1,1000000:	Open valve 6
2,IE21V25.P40000.:	Aspire for cleaning 1
2,OE20V25.D40000.:	Dispense for cleaning 1
2,IE21V25.P40000.:	Aspire for cleaning 2
2,OE20V25.D40000.:	Dispense for cleaning 2
2,IE21V25.P40000.:	Aspire for cleaning 3
2,OE20V25.D40000.:	Dispense for cleaning 3
2,IE21V25.P40000.:	Aspire for cleaning 4
2,OE20V25.D40000.:	Dispense for cleaning 4
1,0:	Close all valves

Annex B. Data card characteristics



Technical Sales

(800) 531-0205
orders@ni.com

[Requirements and Compatibility](#) | [Ordering Information](#) | [Detailed Specifications](#) | [Pinouts/Front Panel Connections](#)
For user manuals and dimensional drawings, visit the product page: [http://ni.com](#)

Last Revised: 2014-10-05 08:01:54.0

M Series Multifunction DAQ for USB - 16-Bit, 250 kS/s, up to 80 Analog Inputs



- Up to 80 analog inputs at 16 bits, 250 kS/s
- Up to 4 analog outputs at 16 bits, 833 kS/s
- Up to 48 TTL/CMOS digital I/O lines (up to 32 hardware-timed at up to 1 MHz)
- Two 32-bit, 80 MHz counter/timers
- Digital triggering supported; power supply included
- NI-PGIA 2 and NI-MCal calibration technology for improved measurement accuracy
- NI signal streaming for 4 high-speed data streams on USB
- NI-DAQmx driver software and LabVIEW SignalExpress LE included

Overview

With recent bandwidth improvements and new innovations from National Instruments, USB has evolved into a core bus of choice for measurement and automation applications. NI M Series devices for USB deliver high-performance data acquisition in an easy-to-use and portable form factor through USB ports on laptop computers and other portable computing platforms. NI created NI signal streaming, an innovative patent-pending technology that enables sustained bidirectional high-speed data streams on USB. The new technology, combined with advanced external synchronization, helps engineers and scientists achieve high-performance applications on USB.

M Series multifunction data acquisition (DAQ) modules for USB are optimized for superior accuracy at fast sampling rates. They provide an onboard NI-PGIA 2 amplifier designed for fast settling times at high scanning rates, ensuring 16-bit accuracy even when measuring all available channels at maximum speed. All externally powered M Series devices have a minimum of 16 analog inputs, 24 digital I/O lines, digital triggering, and two counter/timers. USB M Series devices are ideal for test, control, and design applications including portable data logging, field monitoring, embedded OEM, in-vehicle data acquisition, and academic. NI USB-622x M Series devices have a one-year calibration interval.

[Back to Top](#)

Requirements and Compatibility

OS Information

- Windows 2000/XP
- Windows Vista x64/x86

Driver Information

- NI-DAQmx

Software Compatibility

- ANSI C/C++
- LabVIEW
- Measurement Studio
- SignalExpress
- Visual C#
- Visual Studio .NET

[Back to Top](#)

Comparison Tables

Family	Connector	Analog Inputs	Resolution	Max Rate	Analog Outputs	Resolution	Max Rate	Digital I/O	Counter/Timer
USB-6221	Screw	16 SE/DI	16 bits	250 kS/s	2	16 bits	833 kS/s	24 (8 clocked)	2

Figure 0.1 Data acquisition card datasheet.

Annex C. Equipment information

Equipment	Brand	Model	Serial number	Calibration
Analytical balance	Sartorius	Quintix125D-1S	0034105301	Daily
Copper electrode	Orion	9429SC	Lot HQ1	To use
Cadmium electrode	Orion	9448SC	Lot EO1	To use
Reference electrode	Orion	900200 Sure Flow	Lot DQ1	To use
pH-meter	Crison	GLP 22	025024	Weekly
Star 5 Plus	Thermo	Orion 5 Star	B15811	Not calibrable
Peristaltic pump	Gilson	Minipuls 3	610K5690	Not calibrable
Agitator	SBS	Top Mixer AT-1	135/17/90/12	Not calibrable